

## N O T I C E

THIS DOCUMENT HAS BEEN REPRODUCED FROM  
MICROFICHE. ALTHOUGH IT IS RECOGNIZED THAT  
CERTAIN PORTIONS ARE ILLEGIBLE, IT IS BEING RELEASED  
IN THE INTEREST OF MAKING AVAILABLE AS MUCH  
INFORMATION AS POSSIBLE

**HAMILTON STANDARD**



SVHSR 7226

NASA-CR-160917

(NASA-CR-160917) BREADBOARD SOLID AMINE  
WATER DESORBED CO<sub>2</sub> CONTROL SYSTEM Test  
Report, 1 Sep. 1979 - 30 Jun. 1980 (Hamilton  
Standard, Windsor Locks, Conn.) 59 p  
HC A04/MF A01

N81-18660

Unclas  
41460

CSSL 06K G3/54

**Test Report**

**Breadboard Solid Amine Water Desorbed**

**CO<sub>2</sub> Control System**

**By**

**Arthur K. Colling and  
Mark M. Hultman**

**Prepared Under Contract No. NAS 9-13624**

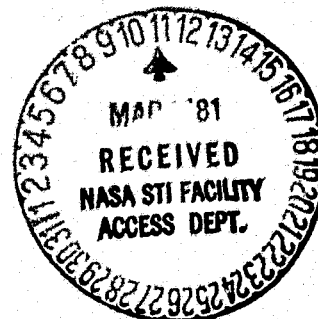
**By**

**Hamilton Standard  
Division of United Technologies Corporation  
Windsor Locks, CT**

**For**

**National Aeronautics and Space Administration  
Lyndon B. Johnson Space Center  
Houston, TX**

**November, 1980**



**Test Report**

**Breadboard Solid Amine Water Desorbed**

**CO<sub>2</sub> Control System**

**By**

**Arthur K. Colling and  
Mark M. Hultman**

**Prepared Under Contract No. NAS 9-13624**

**By**

**Hamilton Standard  
Division of United Technologies Corporation  
Windsor Locks, CT**

**For**

**National Aeronautics and Space Administration  
Lyndon B. Johnson Space Center  
Houston, TX**

**November, 1980**

**Test Report**

**Breadboard Solid Amine Water Desorbed**

**CO<sub>2</sub> Control System**

**By**

**Arthur K. Colling and  
Mark M. Hultman**

**Prepared Under Contract No. NAS 9-13624**

**By**

**Hamilton Standard  
Division of United Technologies Corporation  
Windsor Locks, CT**

**For**

**National Aeronautics and Space Administration  
Lyndon B. Johnson Space Center  
Houston, TX**

**November, 1980**

ABSTRACT

A regenerable CO<sub>2</sub> removal system is being developed for potential use on the Shuttle as an alternate to the baseline lithium hydroxide (LiOH) system. The system is called the solid amine water desorbed, SAWD, CO<sub>2</sub> removal system. It uses a solid amine material to adsorb CO<sub>2</sub> from the atmosphere. The material is regenerated by heating it with steam from a zero gravity water evaporator.

A full sized, thermally representative breadboard canister and a preprototype water evaporator were built and tested to shuttle requirements for CO<sub>2</sub> control. The test program was utilized to evaluate and verify<sup>2</sup> the operation and performance of these two primary components of the SAWD system.

FOREWORD

This report has been prepared by Hamilton Standard, Division of United Technologies Corporation, for the National Aeronautics and Space Administration's Lyndon B. Johnson Space Center in accordance with Contract NAS 9-13624, "Breadboard and Flight Prototype CO<sub>2</sub> and Humidity Control Systems." The report covers work accomplished on the breadboard test program for the Solid Amine Water Desorbed CO<sub>2</sub> Control System between September 1, 1979 and June 30, 1980.<sup>2</sup>

Appreciation is expressed to the Technical Monitor, Mr. Frank Collier of the NASA, Johnson Space Center, for his guidance and advice.

This program was conducted under the direction of Mr. Harlan F. Brose, Program Manager, and Mr. Albert M. Boehm and Mr. Arthur K. Colling, Program Engineers, with the assistance of Mr. Mark M. Hultman, Analysis and Mr. Philip B. Noll, Test Engineering.

TABLE OF CONTENTS

<u>Title</u>	<u>Page No.</u>
Summary	1
Introduction	3
Objectives	4
Conclusions	5
Recommendations	7
Description	8
SAWD Test System	8
Instrumentation	8
Air System Leakage Test	8
Test Canister Background	13
Testing Approach	14
Discussion	16
Bed Differential Pressure Tests	16
Water Evaporator Tests	16
Baseline Performance Tests	23
Parametric Tests	30
Test Results Discussion	35
CO <sub>2</sub> Adsorption on Solid Amine	35
Bed Drying During Cyclic Operation	41
CO <sub>2</sub> Desorption from Solid Amine	41

LIST OF FIGURES

<u>Figure No.</u>	<u>Title</u>	<u>Page No.</u>
Figure 1	SAWD Test Facility Block Diagram	9
Figure 2	SAWD Test System Schematic	10
Figure 3	SAWD Test Canister	11
Figure 4	SAWD Test System CO <sub>2</sub> Leakage	14
Figure 5	SAWD Baseline Testing With Various Beds at 0.4% CO <sub>2</sub>	15
Figure 6	Solid Amine Bed Pressure Drop	17
Figure 7	Water Evaporator Concept	18
Figure 8	Zero Gravity Water Evaporator Differential Pressure	21
Figure 9	SAWD Cyclic Test Runs S-27 - S-36	24
Figure 10	SAWD Cyclic Test Runs S-37 - S-46	25
Figure 11	SAWD Cyclic Test Runs S-47 - S-60	26
Figure 12	SAWD Cyclic Test Runs S-61 - S-65	27
Figure 13	Typical SAWD Test Breakthrough Curve	28
Figure 14	CO <sub>2</sub> Removal Efficiency Versus Time	29
Figure 15	SAWD Cyclic Test Runs S-67 - S-80	31
Figure 16	SAWD Cyclic Test Runs S-81 - S-93	32
Figure 17	SAWD Cyclic Test Runs S-94 - S-101	33
Figure 18	SAWD Cyclic Test Runs S-102 - S-115	34
Figure 19	SAWD Cyclic Test Runs S-116 - S-122	36
Figure 20	Bed Temperature During Adsorption	37
Figure 21	Typical SAWD Test Breakthrough Curve	38
Figure 22	Solid Amine Bed Capacity as a Function of CO <sub>2</sub> Partial Pressure and Cycle Time	39
Figure 23	Effect of Desorb Temperature on Adsorption Breakthrough	41
Figure 24	Effect of Desorption Temperature on Adsorption Performance	42
Figure 25	SAWD Canister Weight Change During Adsorption	43
Figure 26	Effect of CO <sub>2</sub> Loading on Desorption Flow and Time	45
Figure 27	Desorption Mass Characteristic with High CO <sub>2</sub> Loading	46
Figure 28	Desorption Steam Requirements as a Function of Bed Moisture Level	47
Figure 29	Desorption Time Versus Bed Water Loading	48
Figure 30	Percent Moisture Versus Desorption Time	49
Figure 31	Desorption Thermal Characteristic With Low CO <sub>2</sub> Loading	50
Figure 32	Desorption Thermal Characteristic With High CO <sub>2</sub> Loading	51

LIST OF TABLES

<u>Table No.</u>	<u>Title</u>	<u>Page No.</u>
Table 1	Instrumentation List	12
Table 2	Water Evaporator Characteristics	19

### SUMMARY

The Solid Amine Water Desorbed (SAWD) system test program was divided into the major tasks of test system setup, leakage checks and instrumentation calibration; water evaporator tests; solid amine bed differential pressure tests; SAWD system baseline performance tests; and SAWD system parametric tests.

The initial phase of the test setup included building the breadboard solid amine canister and the preprototype zero-gravity water evaporators. The canister was conservatively sized for a four-man metabolic  $\text{CO}_2$  load based on previous small scale test results. It was designed to be thermally representative of a flight unit. Four preprototype water evaporators were constructed. They consisted of tubular electric heating elements inserted into stainless steel tubes. These four units allowed testing of two different heater sizes and four different diametral clearances between the heating elements and the tubes. The SAWD system components were installed in the same test system used previously for HS-C system testing. The baseline and parametric SAWD system cyclic tests were conducted using a closed loop and a  $29.31 \text{ m}^3$  (1035  $\text{ft}^3$ ) chamber as a simulated shuttle cabin volume. Test system leakage tests and instrumentation calibrations were conducted prior to SAWD system testing.

Four zero-gravity water evaporators were tested separately prior to the SAWD system tests. Steady state operation under simulated zero-gravity conditions was demonstrated for various steaming rates within the power capability of the evaporators. Power requirements and differential pressure measurements were taken during the steady state testing. A startup method, which prevents liquid water droplet carryover and limits steam temperature overshoot, was developed. Considering differential pressure through the evaporators, steady state performance, and startup performance, diametral clearances between the heating element and tube of 0.254 to 0.635 mm (0.010 to 0.025 inch) were optimum.

A solid amine bed differential pressure map was generated over a range of flow rates for various bed moisture contents between 14 and 41 percent by weight. For a given flow rate there was only a slight increase in bed differential pressure as moisture content increased within the design range of 20 to 35 percent.

Baseline performance tests established<sub>3</sub> that a 9.53 kg (21.0 lbm) dry weight solid amine bed with 0.99  $\text{m}^3/\text{min}$  (35 CFM) of air flow would maintain an average  $\text{CO}_2$  partial pressure of 3.0 mmHg with a four-man crew. Cyclic equilibrium bed moisture content for the baseline cabin relative humidity is 24 percent by weight for the 96 minute test cycle used.

Parametric tests were conducted to establish the effects of high and low cabin humidity conditions on the SAWD system. Using a fixed operating cycle, with consistently high or consistently low cabin relative humidity, the solid amine bed gradually attained a higher or lower cyclic equilibrium moisture content. CO<sub>2</sub> performance of the solid amine did not degrade, if bed moisture content was maintained between 20 and 35 percent by weight. If the bed moisture content exceeded these limits, CO<sub>2</sub> performance degraded. However, performance recovered when moisture content was restored to the 20 to 35 percent range.

### INTRODUCTION

A regenerable CO<sub>2</sub> control system, called the Solid Amine Water Desorbed (SAWD) system, is being developed for use on the shuttle as an alternate to the baseline lithium hydroxide (LiOH) system. The system uses a solid amine sorbent material to adsorb CO<sub>2</sub> from the cabin atmosphere. The solid amine material is subsequently heated with steam to desorb the CO<sub>2</sub>.

The solid amine material is a polystyrene-divinylbenzene copolymer aminated with diethylenetriamine. The porous substrate exposes an extremely large surface area to the cabin atmosphere.

Per Contract Modification 25S of Contract NAS 9-13624, this test program was designed to evaluate and verify the operation and performance of the two primary components of the SAWD system, the breadboard solid amine canister and the preprototype zero-gravity water evaporator.

### OBJECTIVES

The primary objectives of this test program were to evaluate and verify the operation and performance of the two primary components of the SAWD system, the preprototype water evaporator and the breadboard solid amine canister.

The test program was divided into five parts:

- . Leakage and Instrumentation Calibration
- . Bed Differential Pressure Tests
- . Water Evaporator Tests
- . Baseline Performance Tests
- . Parametric Tests

The objectives of each test phase are listed below:

- . Leakage and Instrumentation Calibration
  - Measure air system leakage
- . Bed Differential Pressure Tests
  - Map bed pressure drop versus air flow rate for various moisture contents
- . Water Evaporator Tests
  - Test operation at various steam flow rates
  - Demonstrate steadystate operation and control
  - Establish and test methods for start-up control
  - Determine the effect of different diametral clearances between the tube and heater element
  - Determine power requirements versus flow rate
  - Establish the relationship between inlet pressure and outlet temperature
  - Establish gravity independence of operation
- . Baseline Performance Tests
  - Determine required air flow rate for the baseline conditions
  - Demonstrate bed water content equilibrium and system CO<sub>2</sub> equilibrium for the baseline conditions.
- . Parametric Tests
  - Evaluate the effects of extremes of cabin temperature and humidity on CO<sub>2</sub> performance and moisture conditioning of the bed.

CONCLUSIONS

1. A 9.53 kg (21.0 lbm) dry weight bed of solid amine with an adsorption flow of 0.99 m<sup>3</sup>/min (35 CFM) and a total cycle time of 96 minutes maintains average cabin CO<sub>2</sub> partial pressure at 3.0 mmHg with a four-man crew.
2. The solid amine material exhibits consistent CO<sub>2</sub> adsorption performance when bed water content is maintained between 20 and 35 percent by weight.
3. When the solid amine bed water content is returned to the 20 to 35 percent range after exceeding this range, CO<sub>2</sub> adsorption performance returns to normal.
4. For the baseline case relative humidity of 50 percent, the solid amine bed cyclic equilibrium water content is 24 percent.
5. If inlet relative humidity during adsorption is continually maintained at the extremes of 27 or 70 percent, the bed cyclic equilibrium water content exceeds the 20 to 35 percent range for optimum CO<sub>2</sub> performance. However, numerous cycles at an extreme relative humidity condition are required before water content exceeds this range.
6. With a fixed steaming rate, the desorption time for a solid amine bed is a strong function of bed water content. Therefore, bed water content for a given SAWD system can be determined from desorption time.
7. During desorption the steam progresses through and heats the solid amine bed in a well-defined wave.
8. During desorption all of the CO<sub>2</sub> which had been adsorbed on the bed is readsorbed and concentrated in the last portion of the bed. When the steam reaches this region of the bed, the CO<sub>2</sub> is pushed out in a high purity wave. The maximum rate at which CO<sub>2</sub> leaves the bed is dependent on the steaming rate.
9. When desorption is performed with the solid amine bed at less than atmospheric pressure, the reduced saturated steam temperature causes some residual CO<sub>2</sub> to be left on the bed.
10. Solid amine bed differential pressure increases only slightly as bed water content varies from 20 to 35 percent by weight.
11. The zero-gravity water evaporator operated well during both start-up and steady state conditions. Insensitivity to gravity was demonstrated during testing by operating the water evaporator in three orthogonal positions.

12. The diametral clearance between the tubular heating element and the tube of a zero-gravity water evaporator should be in the range of 0.254 and 0.635 mm (0.010 and 0.025 inch).
13. Two control methods for steady state operation of the zero-gravity water evaporators were developed.
14. The startup of the zero-gravity water evaporators can be controlled without experiencing any liquid water carryover.

RECOMMENDATIONS

1. Based on the successful results of the breadboard SAWD system test program, a prototype SAWD system should be built and tested.
2. The water evaporator should be attached to the inlet header of the solid amine canister to minimize condensation in the bed inlet header during desorption by preheating the canister header metal.
3. A two bed SAWD system should be investigated. Two beds would provide redundancy and would help to level desorption power usage peaks and minimize variations in cabin CO<sub>2</sub> partial pressure and relative humidity.

## DESCRIPTION

### SAWD Test System

The SAWD system test components were located in the same test facility used for HS-C system testing. A block diagram of the facility is shown in Figure 1. The SAWD test system portion of the block diagram is shown schematically in Figure 2.

Air from the simulated shuttle cabin was ducted to Rig 88 where a blower provided the head for the entire plumbing loop. The air then passed through a series of heat exchangers and electric reheaters, which provided the temperature and humidity conditioning. Since the complete range of desired dry bulb temperatures and dew points was not obtainable with the test rig, the air was conditioned to an equivalent relative humidity. Before the air was directed to the SAWD canister,  $\text{CO}_2$  partial pressure, temperature, dew point, and flow rate were measured. A venturi and valve arrangement in Rig 88 provided for flow measurement and control. A bypass line allowed conditions to be established without flowing through the canister. Excess moisture in the air leaving the SAWD canister was removed by a heat exchanger before the air returned to the simulated shuttle cabin. Also,  $\text{CO}_2$  at the metabolic production rate was fed into the air stream before it returned to the cabin volume.

The breadboard SAWD test canister is shown in Figure 3. The inside diameter is 40.64 centimeters (16 inches), and the maximum bed depth is 22.86 centimeters (9.0 inches). This size accommodated the bed size requirement estimated from earlier small scale testing. The breadboard canister is thermally representative of a flight unit.

### Instrumentation

The parameters measured during testing are shown in the SAWD test system schematic of Figure 2. The instruments used are defined in Table 1.

All instrumentation was calibrated prior to testing by the Hamilton Standard Instrumentation and Metrology Department. Additionally, the  $\text{CO}_2$  analyzers and hygrometer were calibrated before each day of testing.

### Air System Leakage Test

An air system leakage test was conducted to establish the leakage rate of the overall air circuit, including the breadboard system air circuit, Rig 88, the simulated shuttle cabin volume, and all interconnecting plumbing. The results were used to adjust the  $\text{CO}_2$  feed rate to account for losses due to leakage.

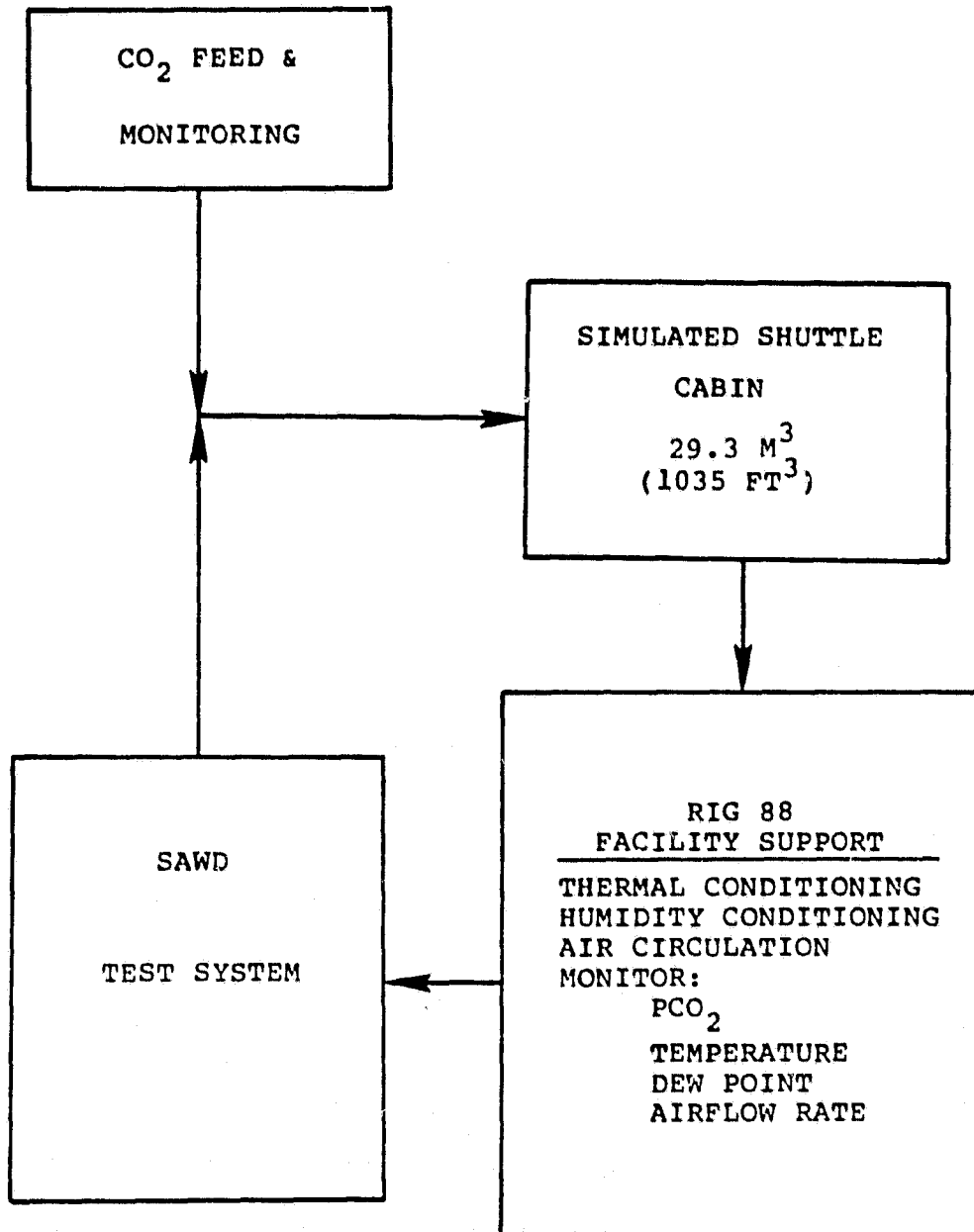


Figure 1  
SAWD TEST FACILITY BLOCK DIAGRAM

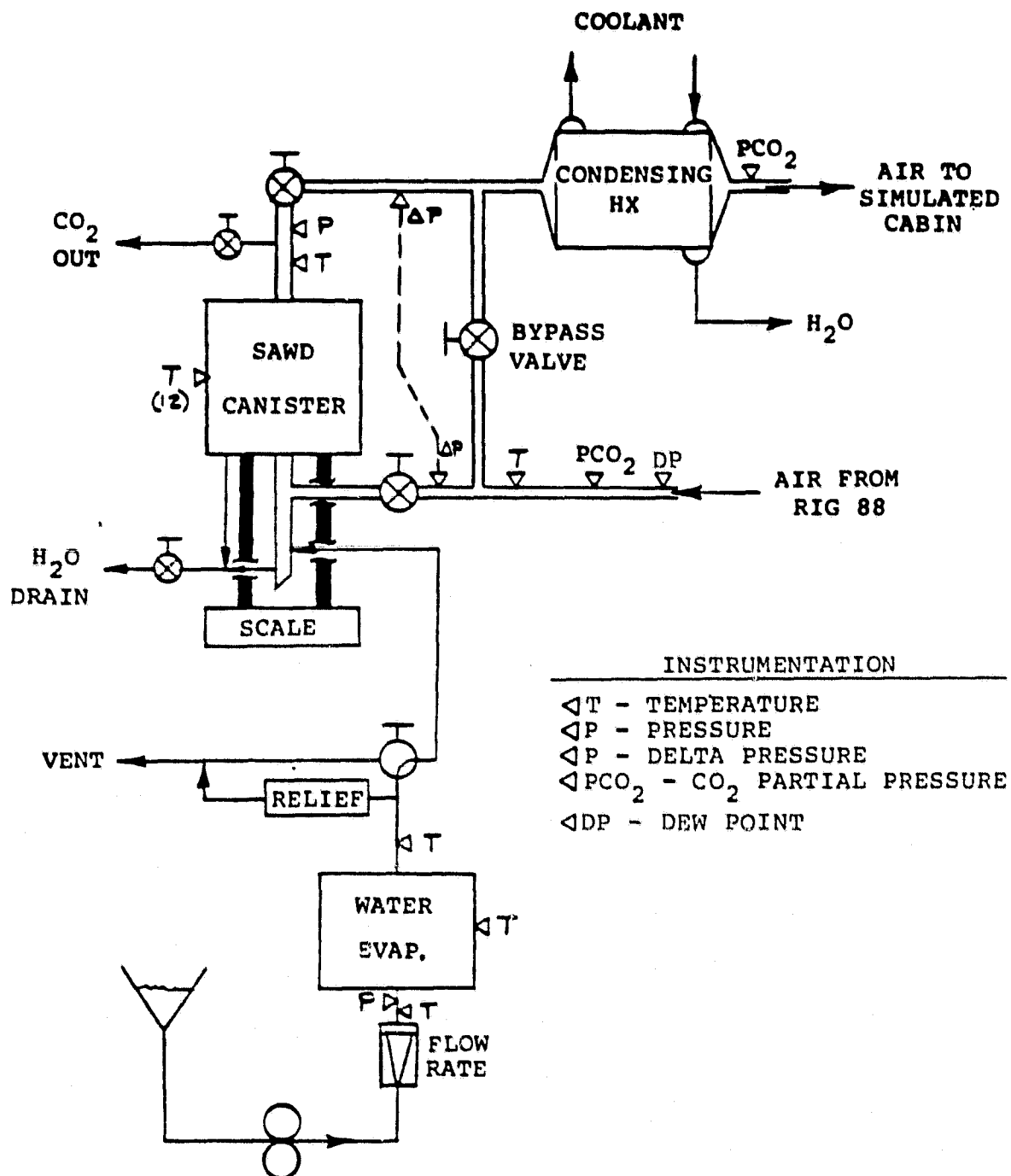


Figure 2  
SAWD TEST SYSTEM SCHEMATIC

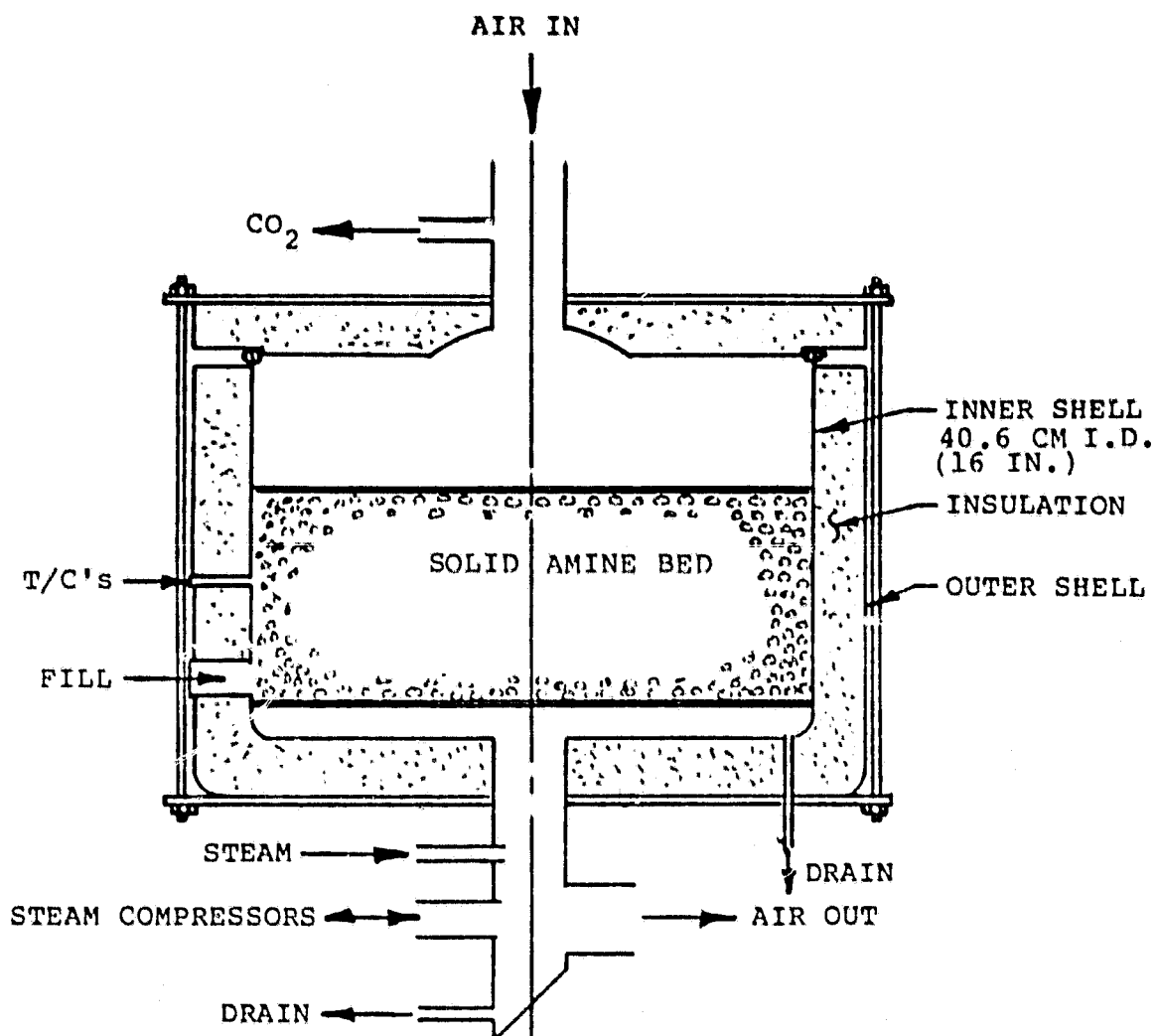


Figure 3  
SAWD TEST CANISTER

Table 1

Instrumentation List

<u>Parameter</u>	<u>Units</u>	<u>Instrument</u>	<u>Range</u>
Rig 88 and SAWD Flow	CFM	Venturi/Manometer	0 to 55 cfm
Makeup CO <sub>2</sub> Flow	lbm/hr	Flow Meter	0 to 1.2 lbm/hr
SAWD Canister Differential Pressure	in. H <sub>2</sub> O	U-tube Manometer	0 to 20 in. H <sub>2</sub> O
SAWD Canister Inlet Dew Point	°F	Hygrometer	-40 to 120°F
SAWD Canister Inlet PCO <sub>2</sub>	volume	Infra-red Analyzer	0-3%
SAWD Canister Outlet PCO <sub>2</sub>	volume	Infra-red Analyzer	0-3%
SAWD Canister Weight	lbm	Scale	0-300 lbm
Makeup CO <sub>2</sub> Weight	lbm	Scale	0-300 lbm
SAWD Canister Outlet Pressure	psia	Gage	0-30 psia
Water Evaporator Inlet Pressure	psia	Gage	0-30 psia
Temperatures Canister Inlet Canister Outlet Water Evaporator Outlet Water Evaporator Inlet Water Evaporator (9) SAWD Canister (12)	°F	Thermocouples	-328 to 752°F
Water Evaporator Feed Flow	lbm/hr	Flow Meter	0-22 lbm/hr

The leakage test was conducted by establishing a known CO<sub>2</sub> concentration in the test system and monitoring the decay<sup>2</sup> in CO<sub>2</sub> concentration while the air circuit was in operation. Figure 4 shows the decay in CO<sub>2</sub> concentration during the test. With an average CO<sub>2</sub> concentration of 3.0 mmHg, 0.4 percent by volume, CO<sub>2</sub> leakage was 0.01331 kg (0.02934 lbm) per 96 minute test cycle<sup>2</sup>. The SAWD canister was bypassed during this test to ensure that no CO<sub>2</sub> would be adsorbed on the bed. The small portion of the system containing the canister had previously been shown to be free of leakage by a vacuum drop test.

### Test Canister Background

The baseline removal capacity for a SAWD system must be 0.254 kg (0.56 lbm) of CO<sub>2</sub> for a four-man crew during a 96 minute orbit. The required solid amine bed size evolved to the final value of 9.53 kg (21 lbm) dry weight during development testing. Figure 5 summarizes this evolution. Based on testing with a 1.81 kg (4 lbm) bed prior to August 1979, the baseline system design was a 14.97 kg (33 lbm) dry weight constrained bed. Airflow was upward through the bed at 1.42 m<sup>3</sup>/min (50 CFM), and steam flow was also upward at 4.31 kg/hr (9.5 lbm/hr). The SAWD test canister was built to these requirements. However, since it was initially filled with solid amine containing 10 percent moisture, the test canister actually held 14.06 kg (31 lbm) of dry solid amine material. As seen in Figure 5, the 14.06 kg (31 lbm) bed at 1.42 m<sup>3</sup>/min (50 CFM) had significantly greater removal capacity than required. Scaling down directly, the new required bed size was 11.34 kg (25 lbm), of dry solid amine and flow direction was changed to down flow to prevent potential channelling. The change in<sub>3</sub> flow direction resulted in improved performance, and at 1.42 m<sup>3</sup>/min (50 CFM) removal capacity was still<sub>3</sub> significantly greater than required. A flow reduction to 0.99 m<sup>3</sup>/min (35 CFM) gave some reduction in bed loading, but a second scaling down of bed weight was necessary for correct sizing. The final system design for the SAWD test program was a 9.53 kg (21 lbm) dry weight, loose filled bed. Air flow was downward at 0.99 m<sup>3</sup>/min (35 CFM), and steam flow was upward at 1.36 kg/hr (3.0 lbm/hr).

### Testing Approach

During the SAWD test program 122 test cycles were run on the 9.53 kg (21 lbm) dry weight bed. The cycles were 96 minutes in length to correspond to one orbit. The target for adsorption time was 52 minutes. However, since required desorption time using a fixed steam flow varied with bed moisture content, adsorption time was made equal to 96 minutes minus desorption time. The first 26 cycles were used to establish and optimize the test procedure. Also bed differential pressure tests and reduced pressure desorption tests were performed during this period. Test cycles 27 to 66 were used to establish the baseline system performance, and cycles 67 to 114 were used for parametric testing. Baseline performance was tested for repeatability during the final eight cycles.

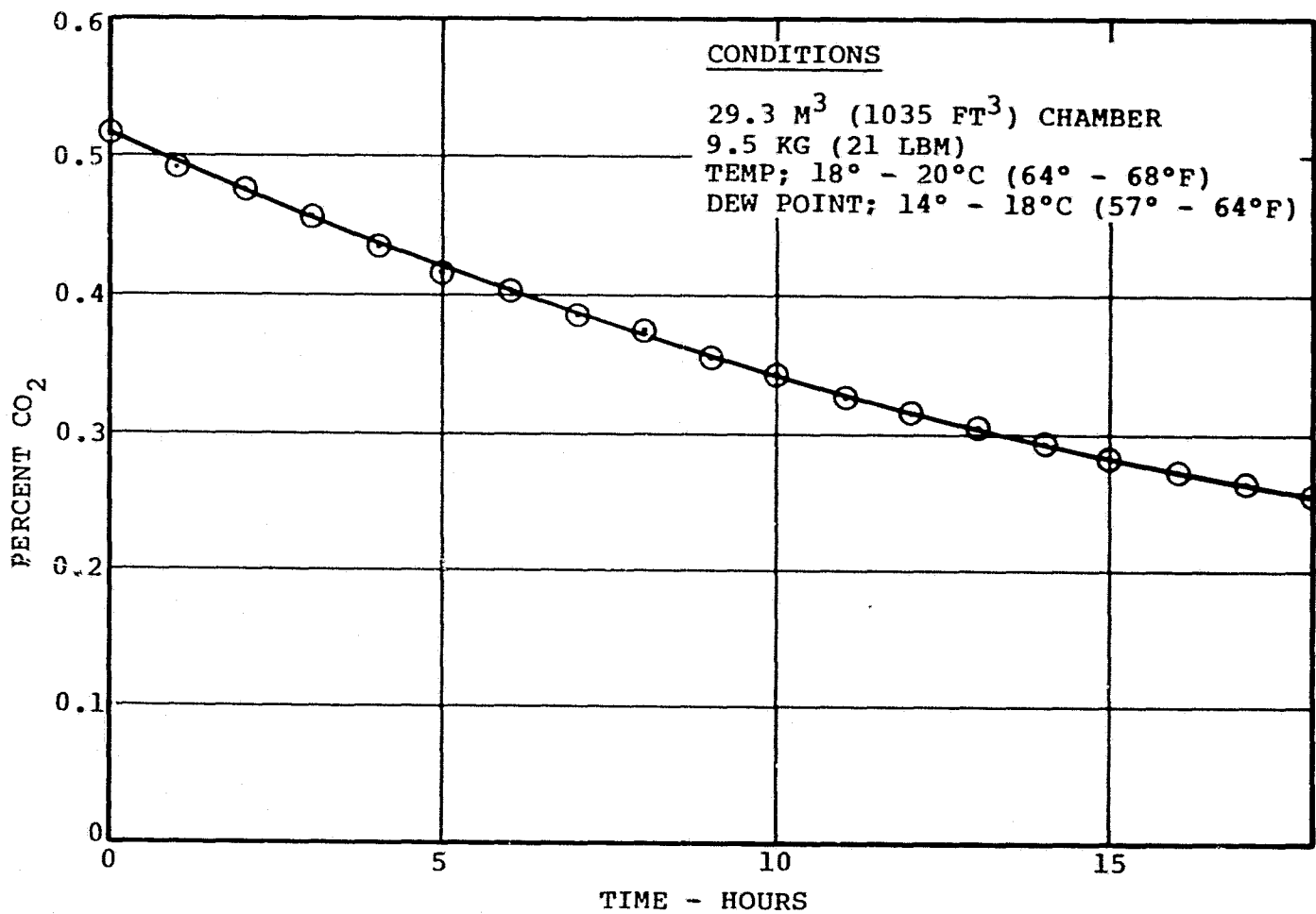


Figure 4  
 SAND TEST SYSTEM CO<sub>2</sub> LEAKAGE

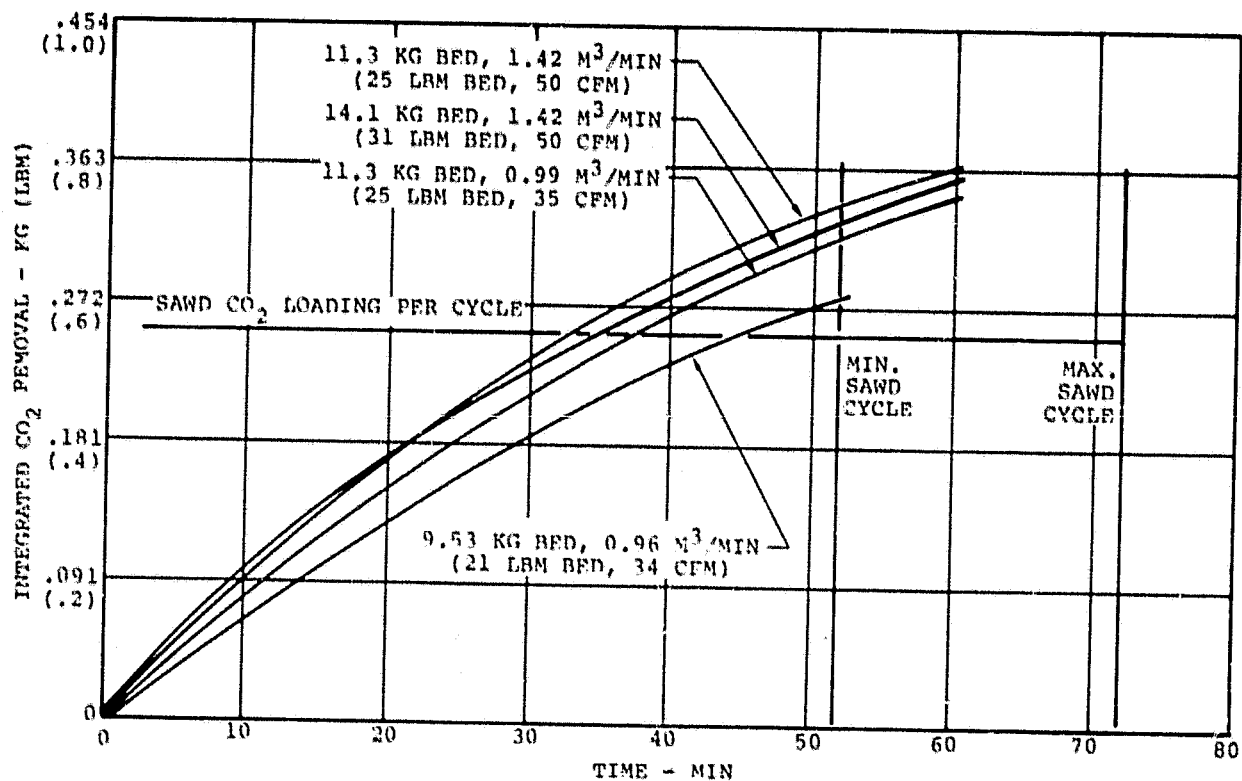


Figure 5  
SAWD BASELINE TESTING WITH VARIOUS  
BEDS AT 0.4% CO<sub>2</sub>

## DISCUSSION

### Bed Differential Pressure Tests

Tests were conducted to map bed differential pressure versus air flow rate over a range of bed water contents. Air flow rate was varied from 0.566 to 1.331 m<sup>3</sup>/min (20 to 47 CFM). Six bed water contents were tested between 14 to 41 percent. The range of 20 to 35 percent bed moisture content is of particular interest, since the solid amine material must be within these limits for proper CO<sub>2</sub> performance. The results are shown in Figure 6.

There is an increase in bed differential pressure as moisture content increases. However, since the solid amine material swells as water is adsorbed, the inter-particle void space grows in proportion to water loading. This tends to limit the bed differential pressure increase with higher water loading.

### Water Evaporator Tests

Preprototype water evaporators were performance tested prior to installation into the SAWD test system. The zero-gravity water evaporator concept is shown in Figure 7. The evaporator consists of a tubular electric heating element inserted into a stainless steel tube. The diametral clearance between the heating element and the tube is 0.254 - 0.635 mm (0.010 - 0.025 inch). The heater and tube lengths are typically 2.54 - 5.08 meters (100 - 200 inches) depending on the required steam production rate. However, once the heating element has been inserted into the tube, the assembly can be bent into a convenient shape. A temperature sensor is installed in contact with the heating element near the steam outlet to provide a control signal. Feedwater to the evaporator is supplied through a flow meter by a variable stroke, piston type metering pump.

Four preprototype zero-gravity water evaporators were performance tested. Three of the evaporators consisted of 1.5875 centimeter (0.625 inch) outside diameter stainless steel tubes with 1.260 centimeter (0.496 inch) diameter tubular electric heating elements inside. Three different wall thickness tubes resulted in three different diametral clearances between the tubes and heating elements. The fourth evaporator was constructed with a 0.9525 centimeter (0.375 inch) outside diameter tube with a 0.6604 centimeter (0.260 inch) diameter heating element. A summary of the water evaporator characteristics is given in Table 2.

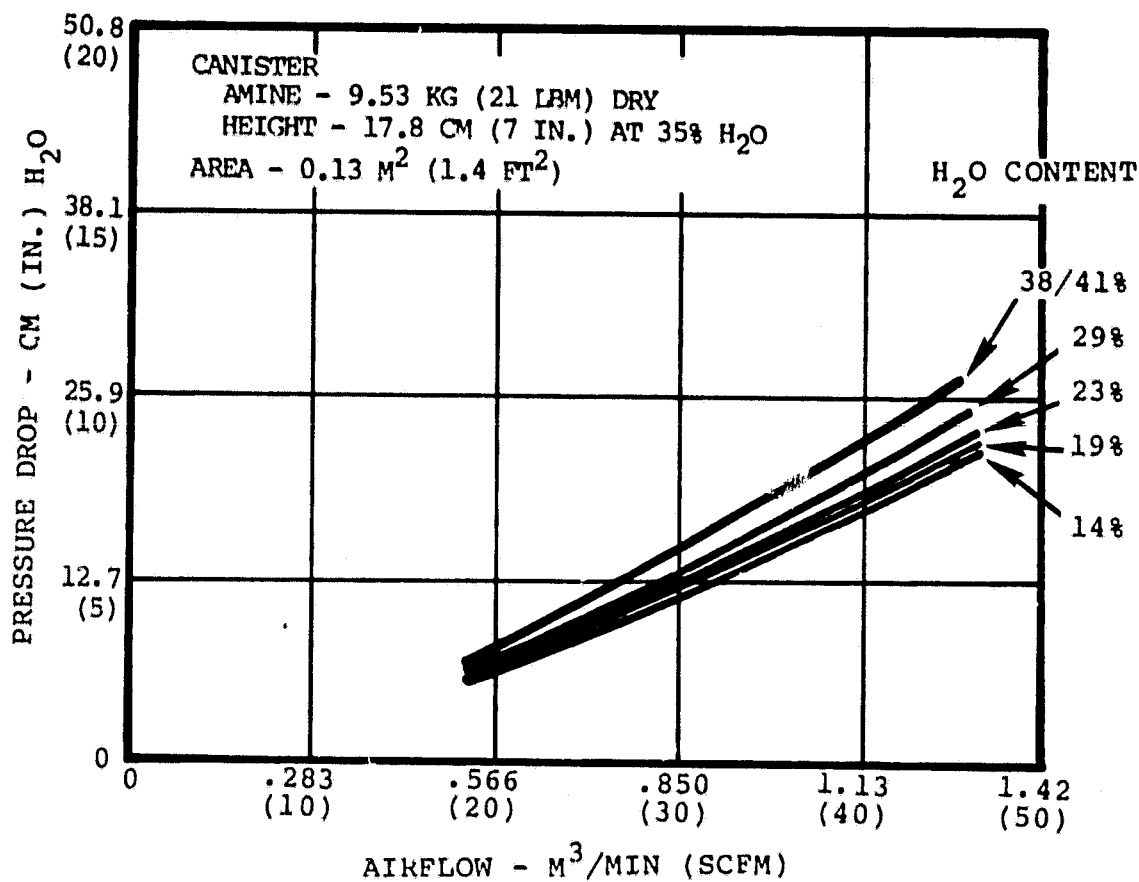


FIGURE 6  
 SOLID AMINE BED PRESSURE DROP

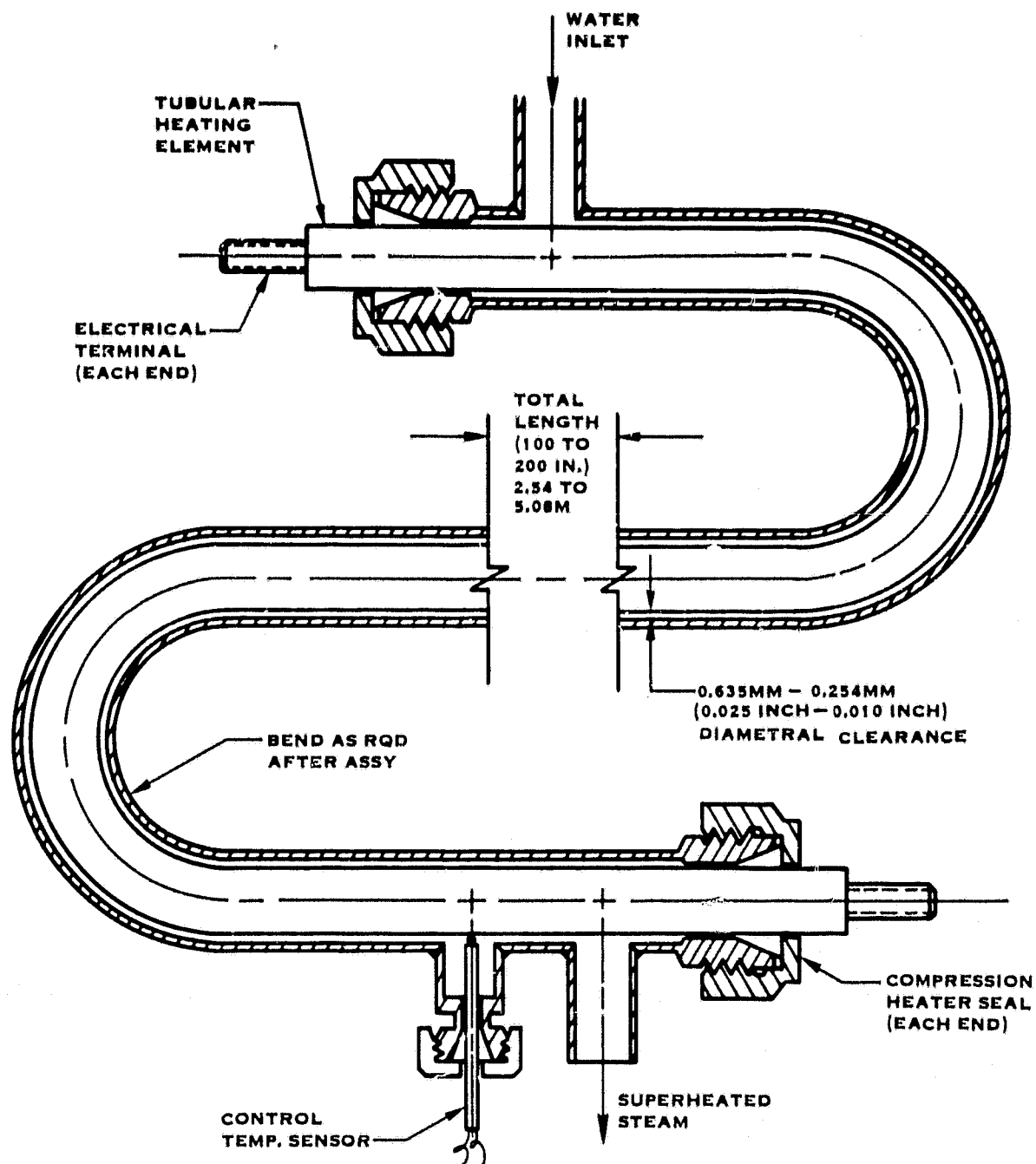


Figure 7  
WATER EVAPORATOR CONCEPT



Table 2  
Water Evaporator Characteristics

Tube O.D. cm. (inch)	Tube Wall Thickness cm. (inch)	Heater O.D. cm. (inch)	Diametral Clearance mm. (inch)	Overall Heater Length cm. (inch)	Heated Length cm. (inch)	Heater Max. Power (KW)
1.5875 (0.625)	0.0889 (0.035)	1.260 (0.496)	0.7493 (0.0295)	307.34 (121)	271.78 (107)	5.0
1.5875 (0.625)	0.1245 (0.049)	1.260 (0.496)	0.3937 (0.0155)	307.34 (121)	271.78 (107)	5.0
1.5875 (0.625)	0.1473 (0.058)	1.260 (0.496)	0.1651 (0.0065)	307.34 (121)	271.78 (107)	5.0
0.9525 (0.375)	0.1245 (0.049)	0.6604 (0.260)	0.2159 (0.0085)	231.14 ( 91)	208.28 ( 82)	2.0

The test system is shown schematically in Figure 2. Support equipment for the evaporator consisted of a metering pump, a flow meter, an electrical controller, a pressure gage, and a thermocouple readout. The metering pump was a Fluid Metering Incorporated model RP-D-0. It was a reciprocating piston pump with a variable stroke. Thermocouples were positioned in contact with the outside of the stainless steel tube at nine locations along the evaporator. Two thermocouples were placed in contact with the heating element. One was located near the middle of the evaporator, and the other was near the steam outlet. This latter thermocouple was used as a controller input. Since the evaporator outlet was vented to atmosphere, the pressure gage at the inlet indicated pressure drop through the evaporator.

Figure 8 shows the relationship between pressure drop through the evaporators and steam flow rate. Pressure drop is a function of both evaporator diameter and diametral clearance between the heating element and the tube, since both of these factors affect the flow area. Four evaporators with diametral clearances between the heating element and tube ranging from 0.1651 mm (0.0065 inch) to 0.7493 mm (0.0295 inch) were tested. As expected, larger clearances resulted in smaller differential pressure drops through the evaporators. Steady state performance was satisfactory for all evaporators tested, except the 0.1651 mm (0.0065 inch) clearance evaporator had a pressure drop which was too high for safe operation with the test system. The medium clearance evaporator, 0.3937 mm (0.0155 inch), was easier to control during startup without experiencing liquid water carryover.

During the remainder of the SAWD test program the 0.9525 centimeter (0.375 inch) diameter, two KW evaporator was used for steam desorption of the SAWD beds, since its size matched the steam flow rates needed. Over 200 hours of operating time was completed with this evaporator with no performance degradation.

Water evaporators were successfully tested over the range of flow rates from 0.59 kg/hr (1.30 lbm/hr) to 4.20 kg/hr (9.25 lbm/hr). These limits are of no particular significance, except that they were within the capability of the test equipment. Water evaporators of this design can be built for any steam flow rate corresponding to available heater element and tube size combinations.

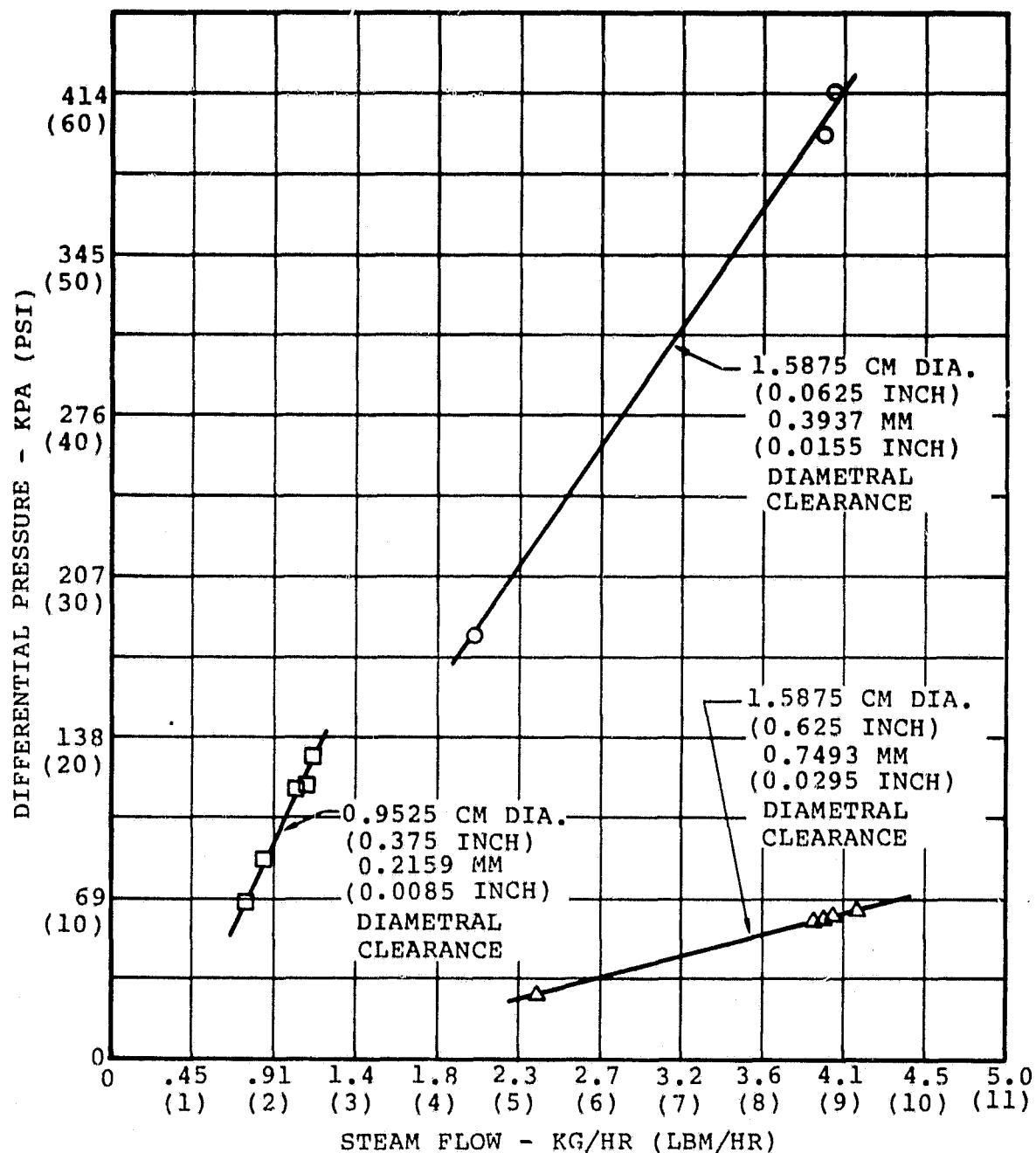


Figure 8  
ZERO GRAVITY WATER EVAPORATOR  
DIFFERENTIAL PRESSURE

Steady state operation at numerous steaming rates was demonstrated. With proper power control, there was no liquid water carryover, and the degree of superheat was easily controlled. Two control methods were successfully tested for steady state operation. With the first method a fixed heater power was cycled on and off based on a selected control sensor temperature. With the second method voltage to the heater was adjusted based on a selected control sensor temperature.

The objective of startup control was to prevent liquid water droplets from being carried with the steam during evaporator heat-up. If the pump and heater were energized simultaneously, some liquid water was forced out with the initial steam flow. If the heating element was preheated before the pump was started, water carryover was initially prevented, but there was a temporary instability in steam temperature. Typically, steam temperature first overshot and then undershot the desired temperature before stabilizing. Often some water droplet carryover was experienced during the low temperature swing. The above problems were eliminated with the following startup method. The heating element was preheated to a specified temperature. When the pump was started, the heater was deenergized until outlet steam temperature peaked. Then, heater power was returned to its operating level.

For all evaporators tested average power consumption was 0.761 KWH/kg (0.345 KWH/lbm) of steam. This value corresponded to a 5.6 percent inefficiency due to heat losses to ambient. Since heat loss to ambient was independent of steam flow rate, the inefficiency percentage was slightly less at higher steaming rates. Power for the metering pump was not included in these values.

Inlet pressure and outlet temperature were not directly related. Inlet pressure was primarily a function of diametral clearance between the tube and heating element and steam flow rate. Outlet temperature was primarily a function of input power.

Operation of the water evaporators was demonstrated to be insensitive to gravity orientation. Evaporators were operated in both startup and steady state modes in three orthogonal positions. No differences were seen in either performance or operating characteristics. Therefore, the performance should not be affected by zero-gravity.

### Baseline Performance Tests

The breadboard SAWD system was tested to verify baseline performance under the following conditions:

Parameter	Requirement
Inlet Air Temperature	21.11°C (70°F)
Inlet Air Dew Point	10°C (50°F)
Air Flow Rate	0.99 m <sup>3</sup> /min (35 CFM)
CO <sub>2</sub> Flow Rate	0.159 kg/hr (0.35 lbm/hr)
CO <sub>2</sub> Level (Max. Average)	3.0 mmHg
Adsorb and Desorb Cycle	96 minutes

Since the required temperature and dew point could not be obtained with the test system, it was agreed with the NASA technical monitor that temperature and dew point could be flexible, if the correct relative humidity was maintained in the canister inlet air flow. The CO<sub>2</sub> flow rate used in the test corresponds to the nominal four-man metabolic rate of 0.957 kg (2.11 lbm) of CO<sub>2</sub> per man-day. The actual CO<sub>2</sub> flow rate used during the test was increased by 0.0083 kg/hr (0.0183 lbm/hr) to account for air system leakage. CO<sub>2</sub> feed rate was constant during each test cycle, and the test chamber CO<sub>2</sub> level was allowed to vary. The test plan specified varying air flow rate as necessary to maintain an average test chamber CO<sub>2</sub> level of 3.0 mmHg. Thus, the required baseline system air flow could be determined. Once the baseline air flow rate was established, test cycles were run using the established air flow value until CO<sub>2</sub> performance and bed water content equilibrium could be demonstrated.

Figures 9 through 12 provide a summary of the system performance during the baseline test cycles, S-27 through S-65. The data for test cycle S-66 was not included due to a rig problem. The figures give test conditions, test chamber CO<sub>2</sub> partial pressure, and bed moisture content. It should be noted that since the test volume was only approximately half the size of an actual shuttle cabin, the CO<sub>2</sub> partial pressure variation during each test cycle was twice as large as the variation in an actual shuttle vehicle.

As seen in Figures 9 through 12, an average test chamber CO<sub>2</sub> partial pressure of 3.0 mmHg, 0.4 percent by volume, was maintained with the 0.99 m<sup>3</sup>/min (35 CFM) air flow rate. Consequently, no air flow rate variations were necessary to establish the baseline value. The test chamber and canister outlet CO<sub>2</sub> partial pressures are shown in Figure 13 for a typical adsorption cycle. Carbon dioxide removal efficiency for the same cycle is shown in Figure 14.

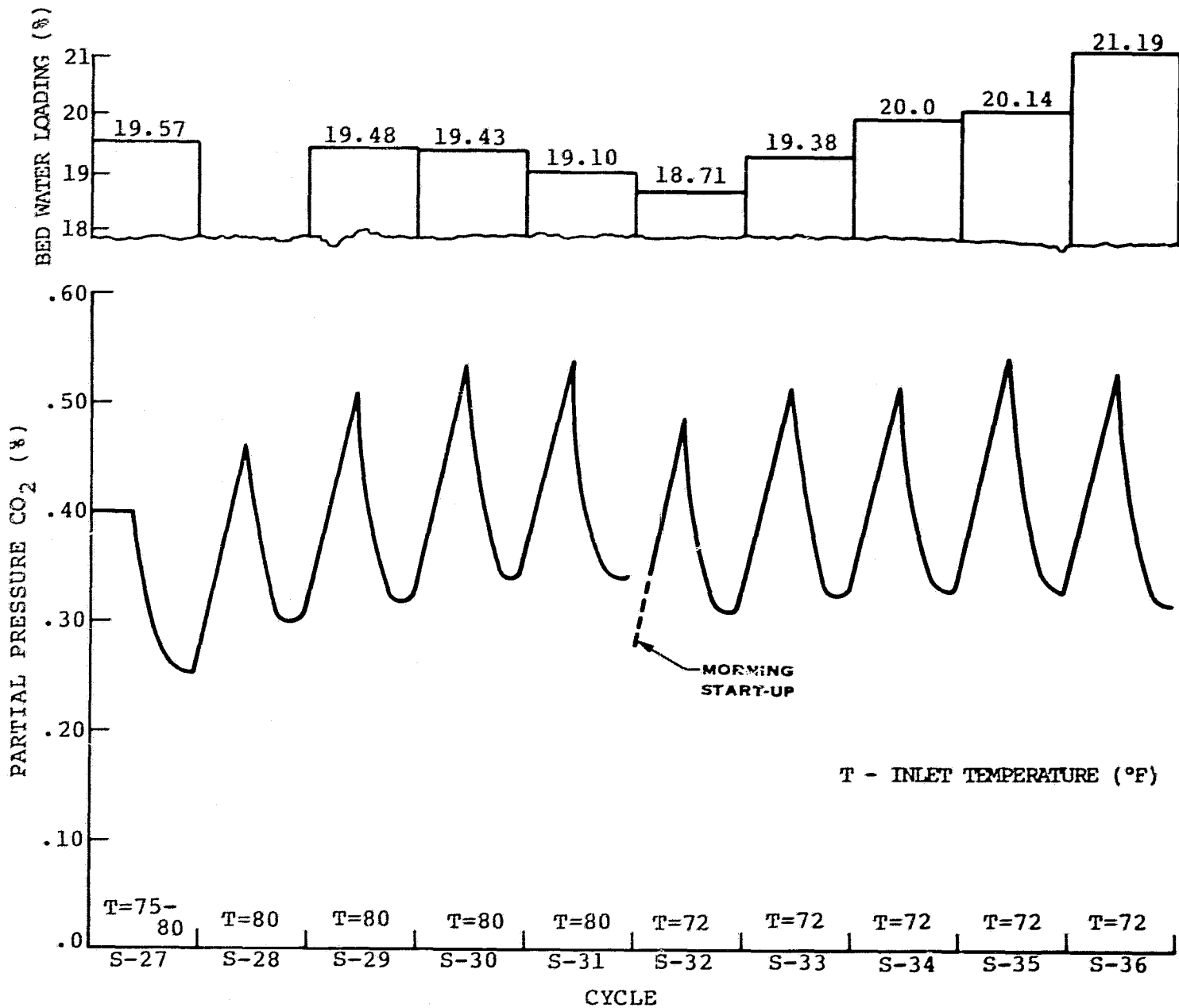
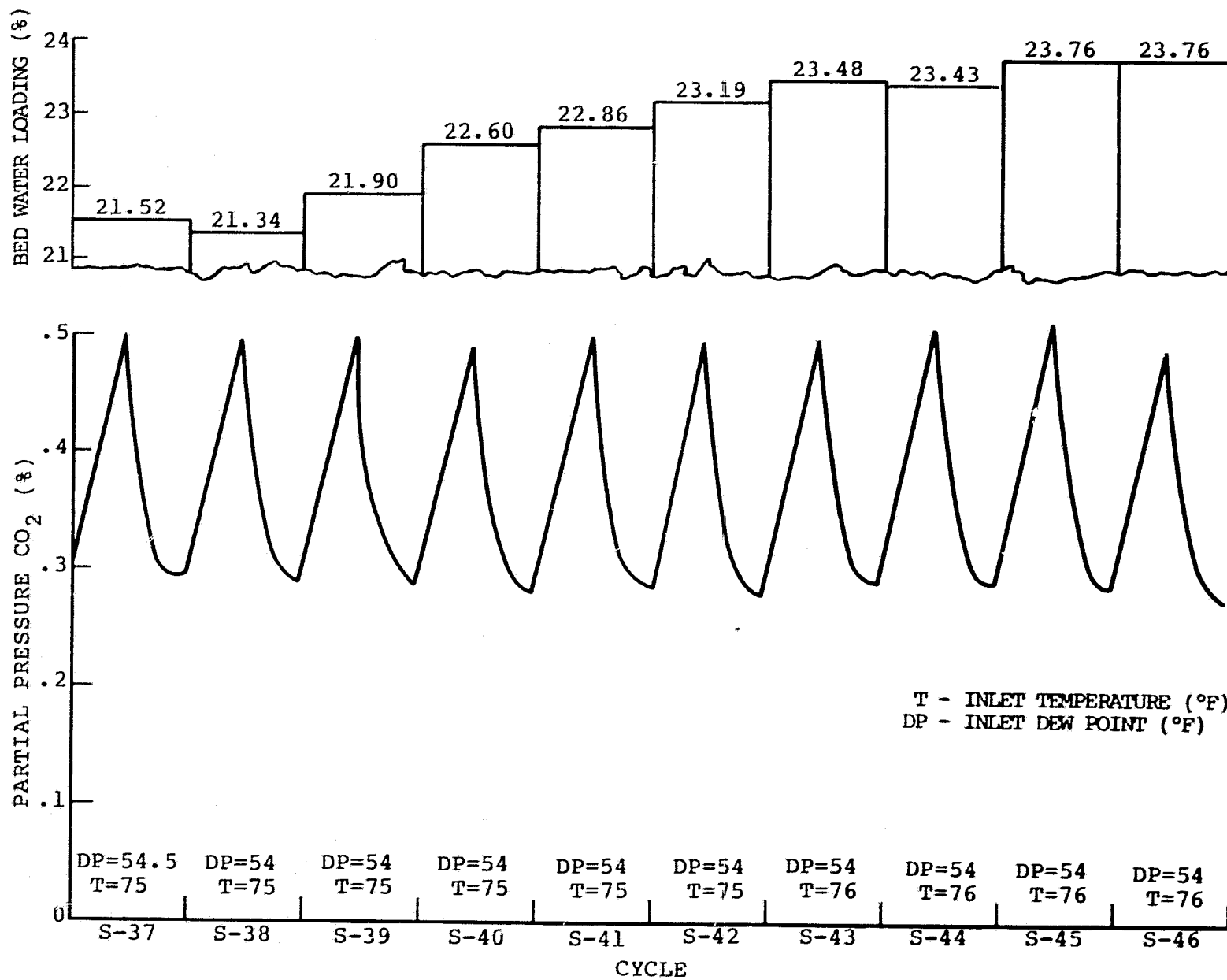


Figure 9  
 SAND CYCLIC TEST RUNS S-27 - S-36



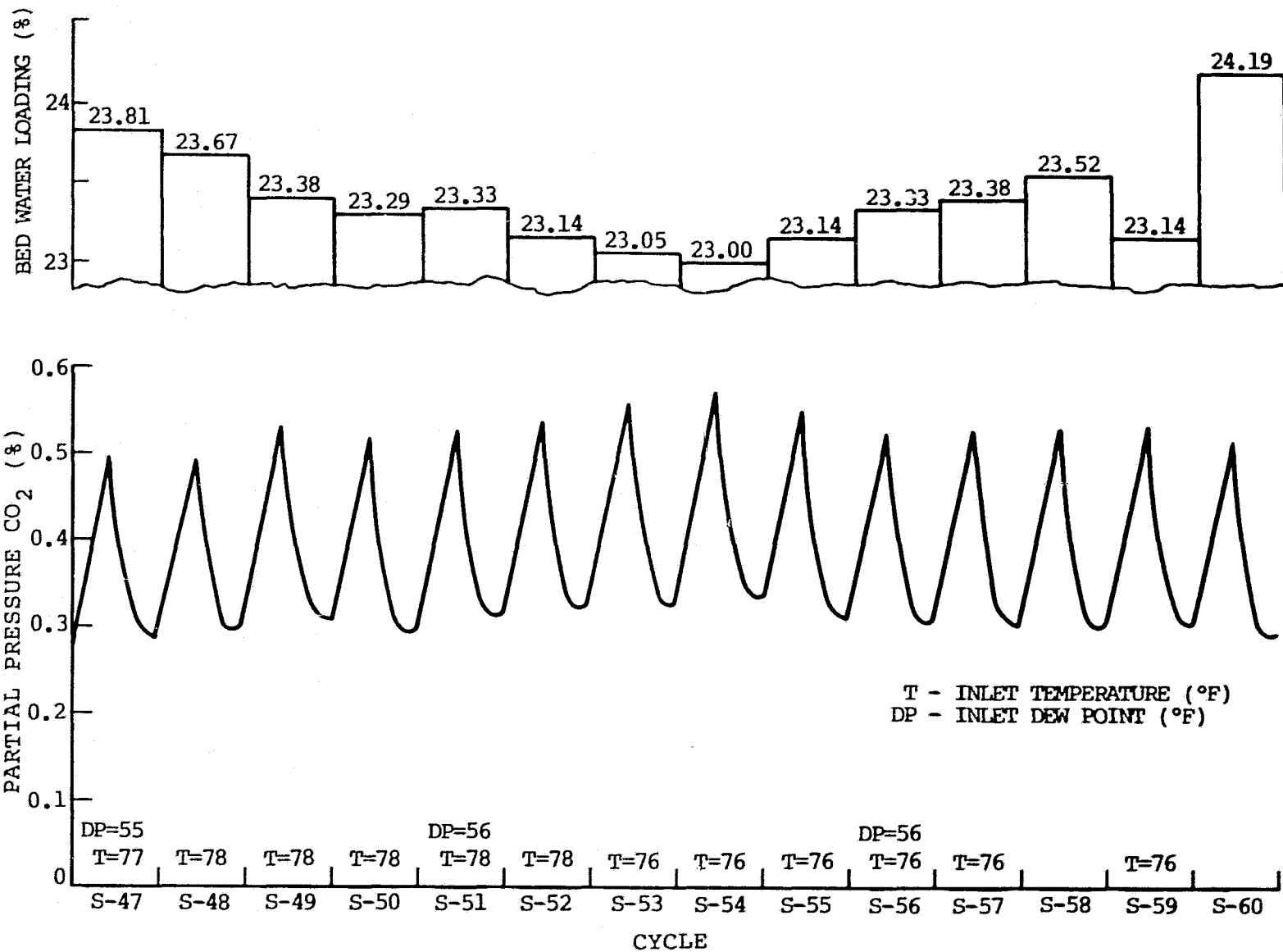


Figure 11  
 SAND CYCLIC TEST RUNS S-47 - S-60

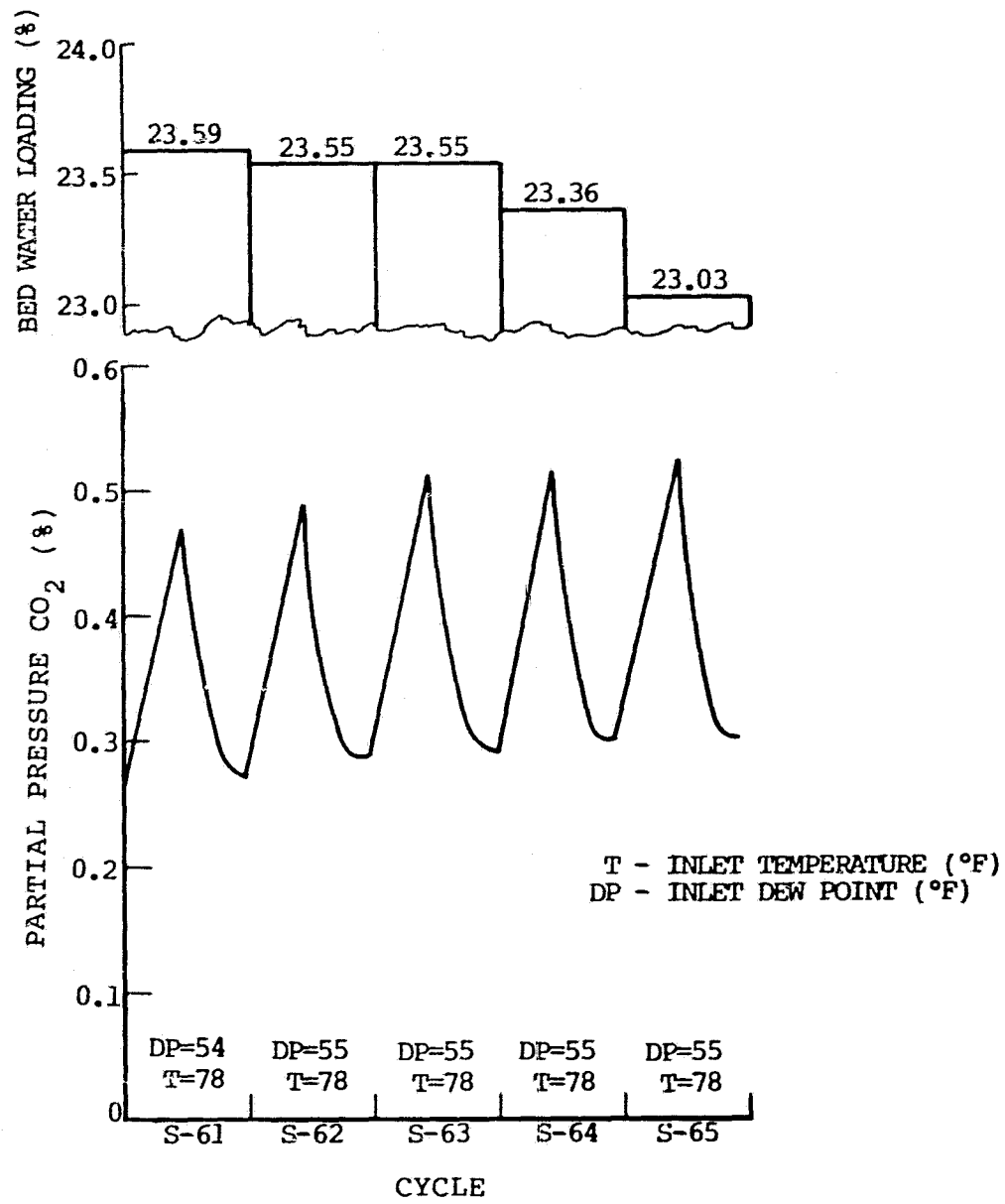


Figure 12  
 SAWD CYCLIC TEST RUNS S-61 - S-65

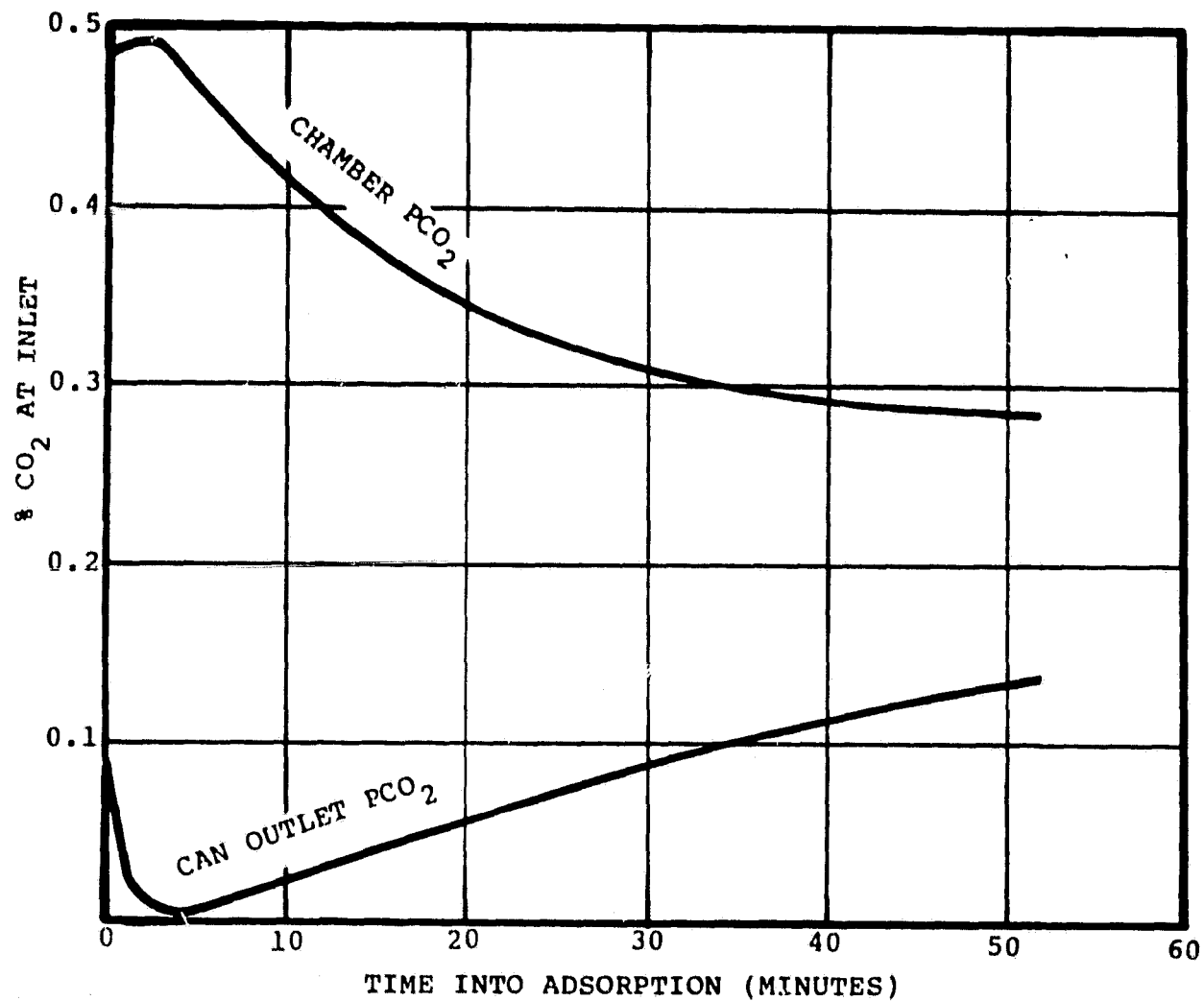


Figure 13  
TYPICAL SAWD TEST BREAKTHROUGH CURVE

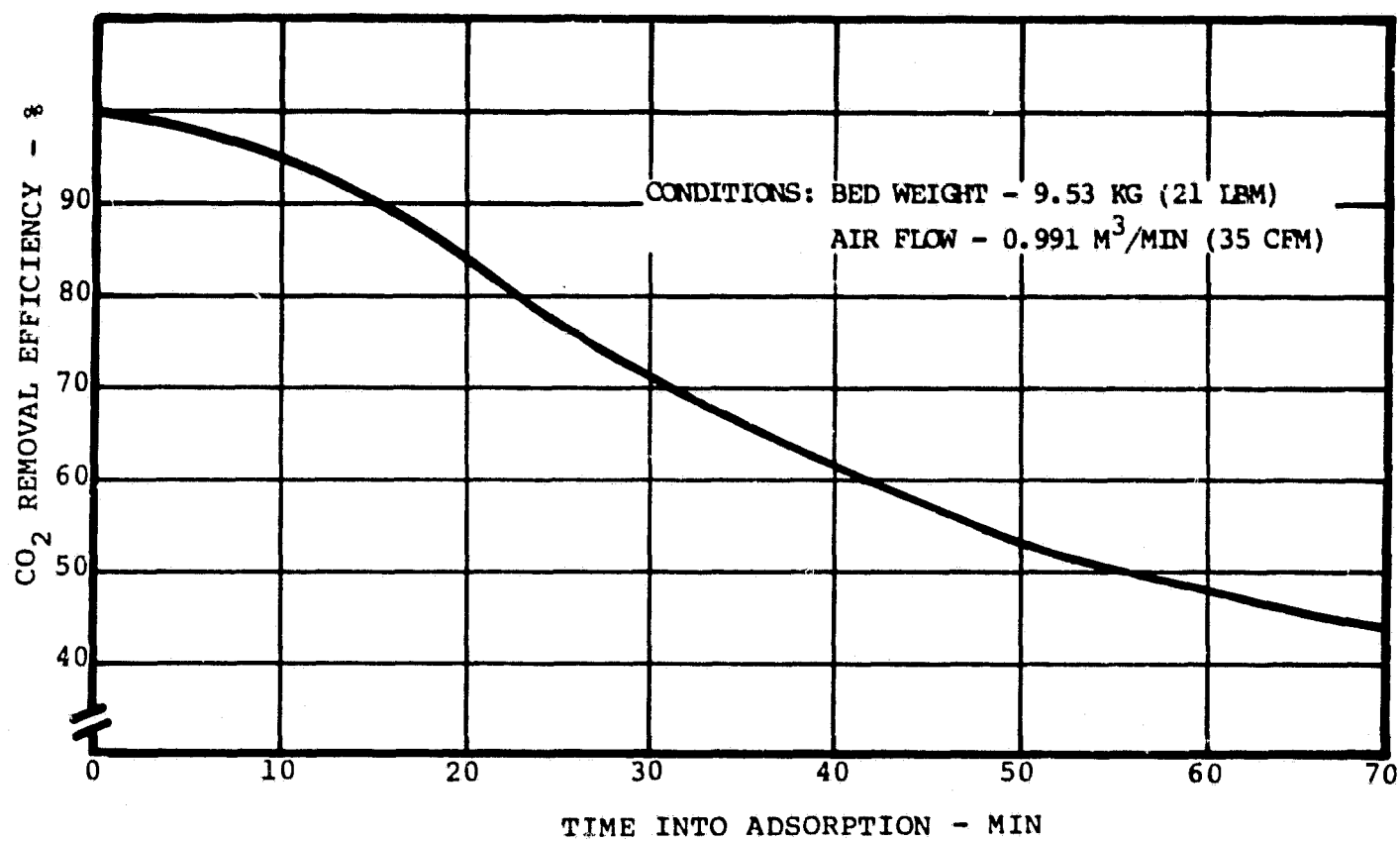


Figure 14  
CO<sub>2</sub> REMOVAL EFFICIENCY VERSUS TIME

Bed moisture content cyclic equilibrium for the baseline conditions was reached by test cycle S-43. This equilibrium value, approximately 24 percent by weight, was maintained for the remaining 22 cycles of the baseline tests. Minor moisture content variations from cycle to cycle are attributable to similar variations in inlet air relative humidity.

### Parametric Tests

The effect of off-design cabin conditions on the SAWD system was tested per the following table:

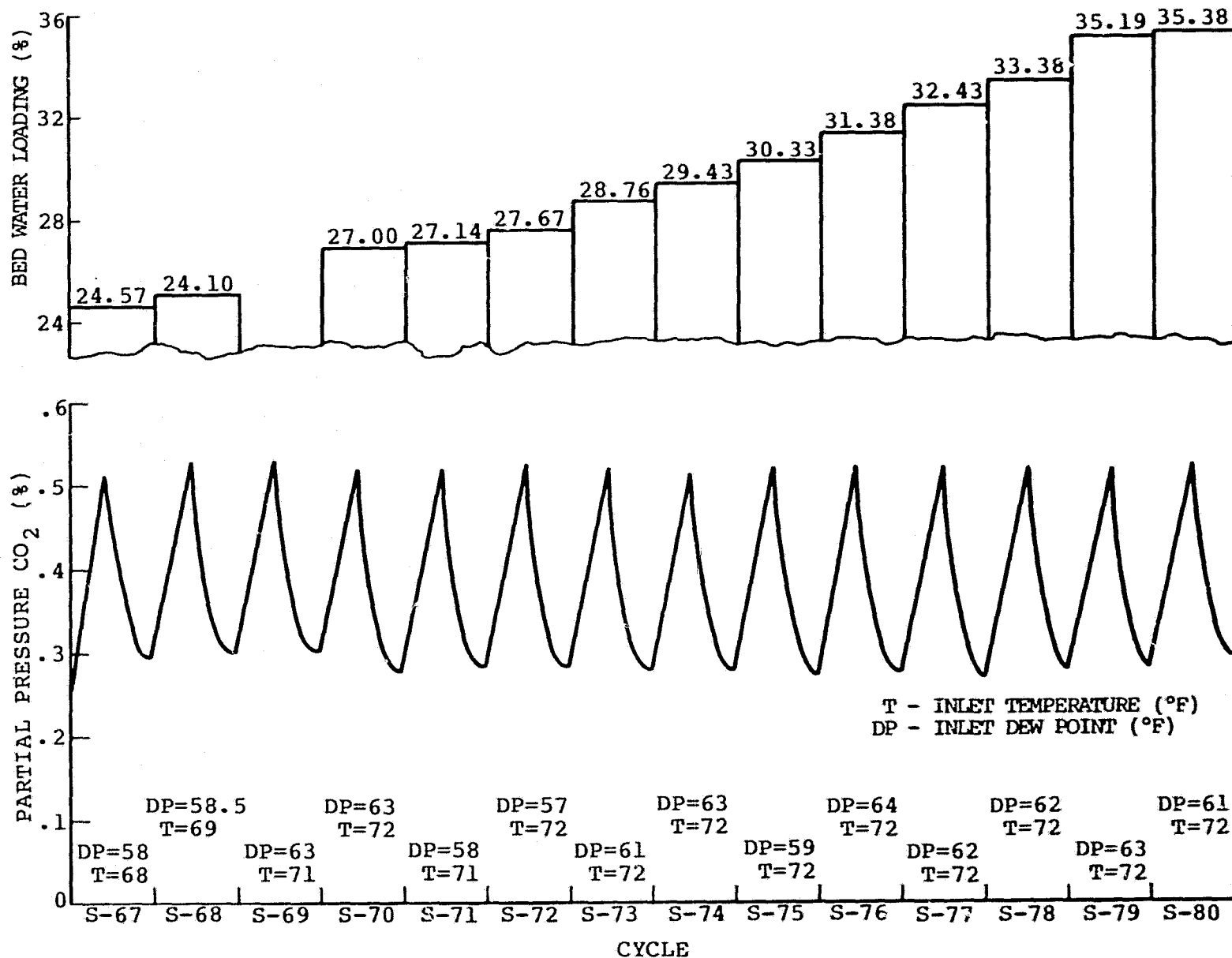
<u>Test</u>	<u>Air Temp.</u> °C (°F)	<u>Air D/P</u> °C (°F)	<u>Air Flow*</u> m <sup>3</sup> /min (CFM)	<u>CO<sub>2</sub> Flow</u> kg/hr (lbm/hr)
high R.H.	21.11 (70)	15.56 (60)	0.99 (35)	0.159 (0.35)
low R.H.	26.67 (80)	6.11 (43)	0.99 (35)	0.159 (0.35)

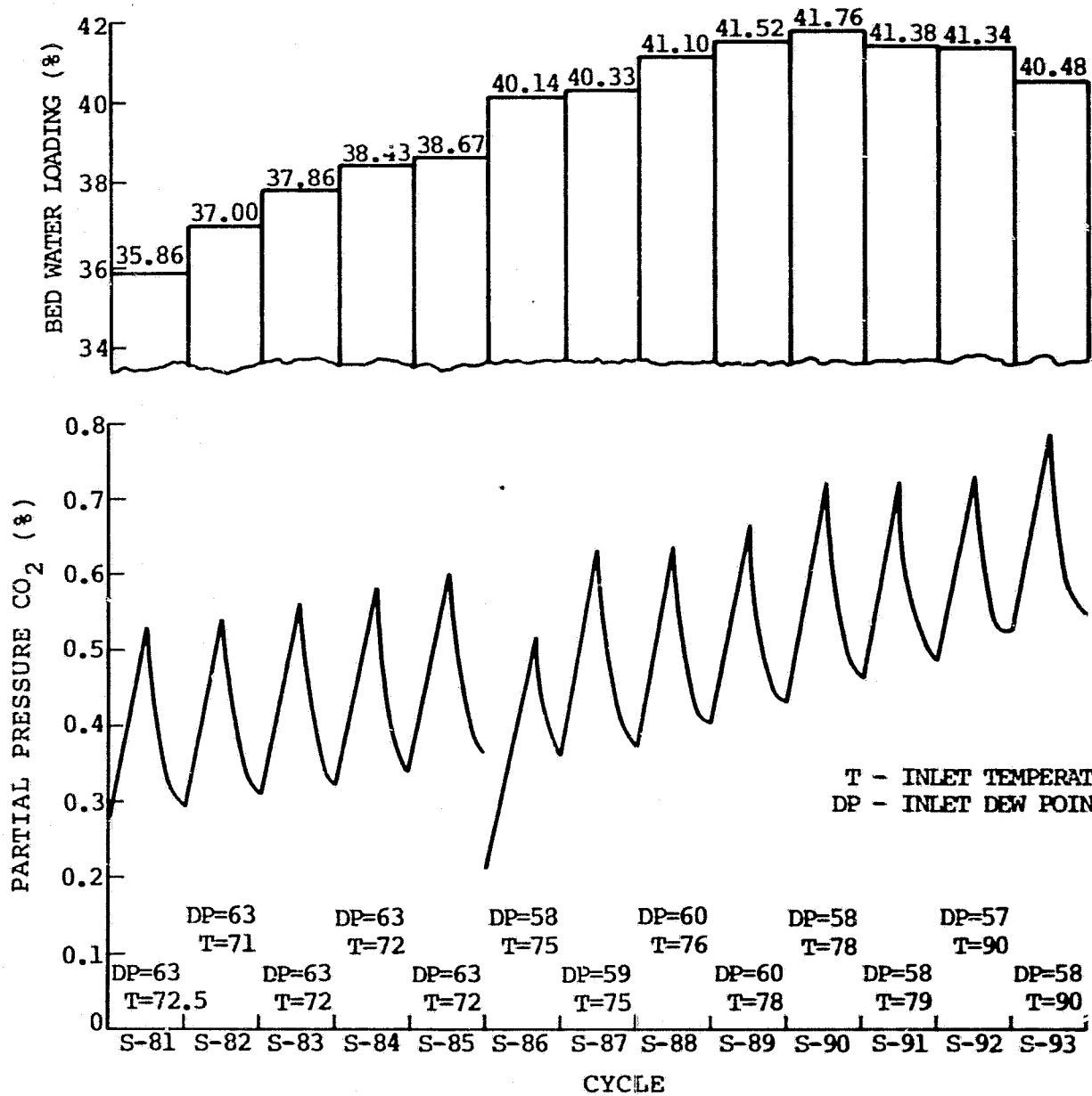
\*The air flow rate established during baseline testing was used.

These tests were utilized to determine the effects of extremes in cabin temperature and humidity on the CO<sub>2</sub> performance and moisture conditioning of the bed. The actual CO<sub>2</sub> flow rate used during the tests was increased by 0.0083 kg/hr (0.0183 lbm/hr) to account for air system leakage. As in the baseline performance tests, the temperature and dew point of the inlet air was flexible, if the correct relative humidity was maintained.

Figures 15 through 18 provide a summary of the system performance during the parametric test cycles, S-67 through S-115. The figures give test conditions, test chamber CO<sub>2</sub> partial pressure, and bed moisture content.

Cyclic testing with high relative humidity inlet air was conducted during test cycles S-67 to S-90. Bed moisture content gradually increased to 35 percent by weight by test cycle S-80. CO<sub>2</sub> performance did not degrade during this moisture content transient. After test cycle S-80, due to the high bed water content, desorption time with a fixed steaming rate exceeded 44 minutes. Therefore, to maintain the 96 minute cycle time, adsorption time was reduced below 52 minutes. The shorter adsorption times reduced drying ability, and the bed moisture content increased to 42 percent by cycle S-90. Also as seen in Figures 16 and 17, CO<sub>2</sub> performance began to degrade when bed moisture content increased above 35 percent after cycle S-80. Inlet air relative humidity was reduced for test cycles S-92 and S-93. Bed moisture content started to decrease; however, numerous cycles would have been necessary to reduce the moisture content significantly. Therefore, the bed was dried to 30 percent





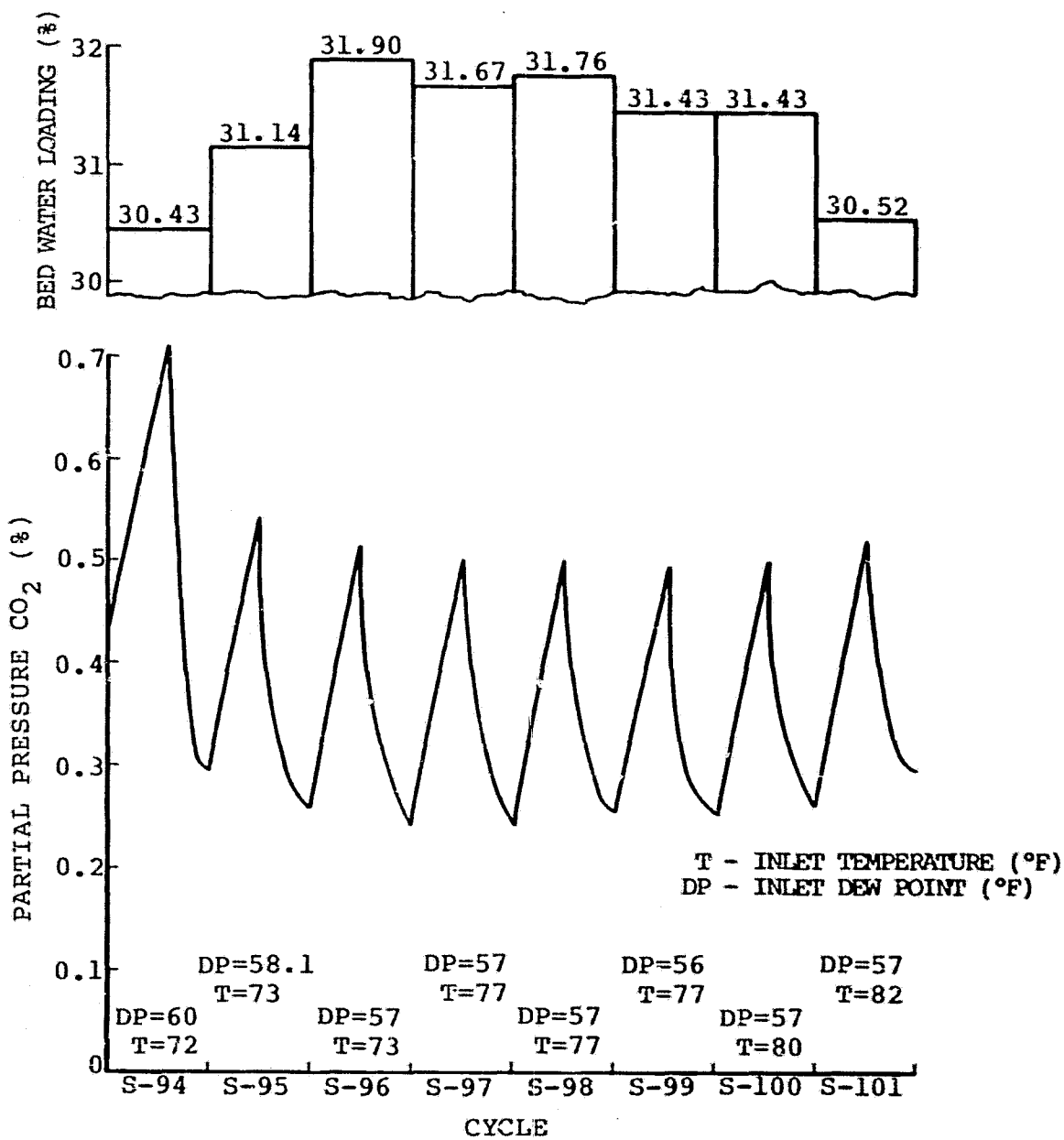
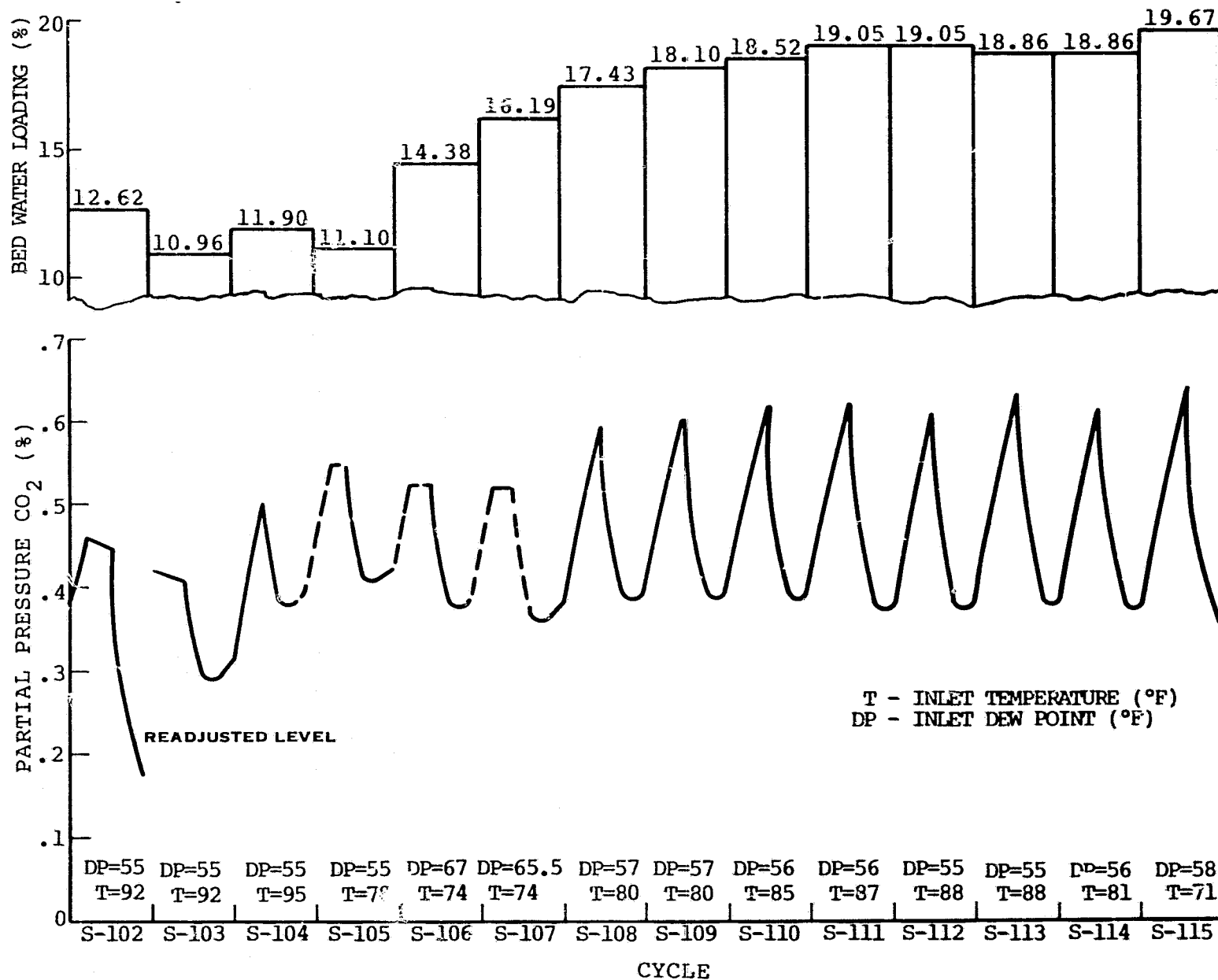


Figure 17  
 SAWD CYCLIC TEST RUNS S-94 - S-101



water content with a continuous dry air flow before the next test cycle. Test cycles S-94 to S-101 were run using near baseline test conditions. Bed moisture content fluctuated near 30 percent. Figure 17 shows that CO<sub>2</sub> performance returned to that experienced during baseline testing, when the bed was dried below 35 percent water content.

Cyclic testing with low relative humidity was conducted during test cycles S-102 to S-114. Refer to Figure 18. The bed water content was reduced to 12 percent by weight using dry air flow prior to test cycle S-102. During test cycles S-102 through S-104, canister inlet air relative humidities averaging 28 percent were used, and bed water content remained between 11 and 12 percent. The CO<sub>2</sub> feed was intentionally retarded during these tests. It was desired to maintain a reasonable system CO<sub>2</sub> level of approximately 3 to 4 mmHg, and the bed breakthrough profile showed predictable degradation at this low moisture level. Higher inlet relative humidities were used for the next five test cycles, S-105 to S-109, and bed water content was increased to the 18 to 19 percent range. However, CO<sub>2</sub> performance remained degraded during these tests. For test cycles S-110 to S-114 average canister inlet relative humidities of 35 percent caused bed water content to remain stable in the 18 to 19 percent range. Carbon dioxide performance continued to be slightly degraded with an average test chamber CO<sub>2</sub> partial pressure of 3.8 mmHg, 0.5 percent CO<sub>2</sub> by volume. For the final eight cycles of the test program, average canister inlet relative humidity was 60 percent, which caused bed water content to increase to 24 percent by weight. As seen in Figure 19, baseline CO<sub>2</sub> performance was restored after bed water content increased above the 20 to 21 percent range.

### Test Results Discussion

#### CO<sub>2</sub> Adsorption On Solid Amine

Adsorption of CO<sub>2</sub> on a solid amine bed begins immediately when a hot bed is returned to adsorption after being steam desorbed. The rapid cooling in the front of the bed, shown in Figure 20, allows adsorption to begin. This is shown by the typical adsorption breakthrough curve of Figure 21.

Solid amine capacity for CO<sub>2</sub> increases significantly as CO<sub>2</sub> partial pressure increases. Figure 22, which was generated by a computer simulation based on available data points, shows the cyclic CO<sub>2</sub> loading on solid amine versus CO<sub>2</sub> partial pressure for various adsorption cycle times.

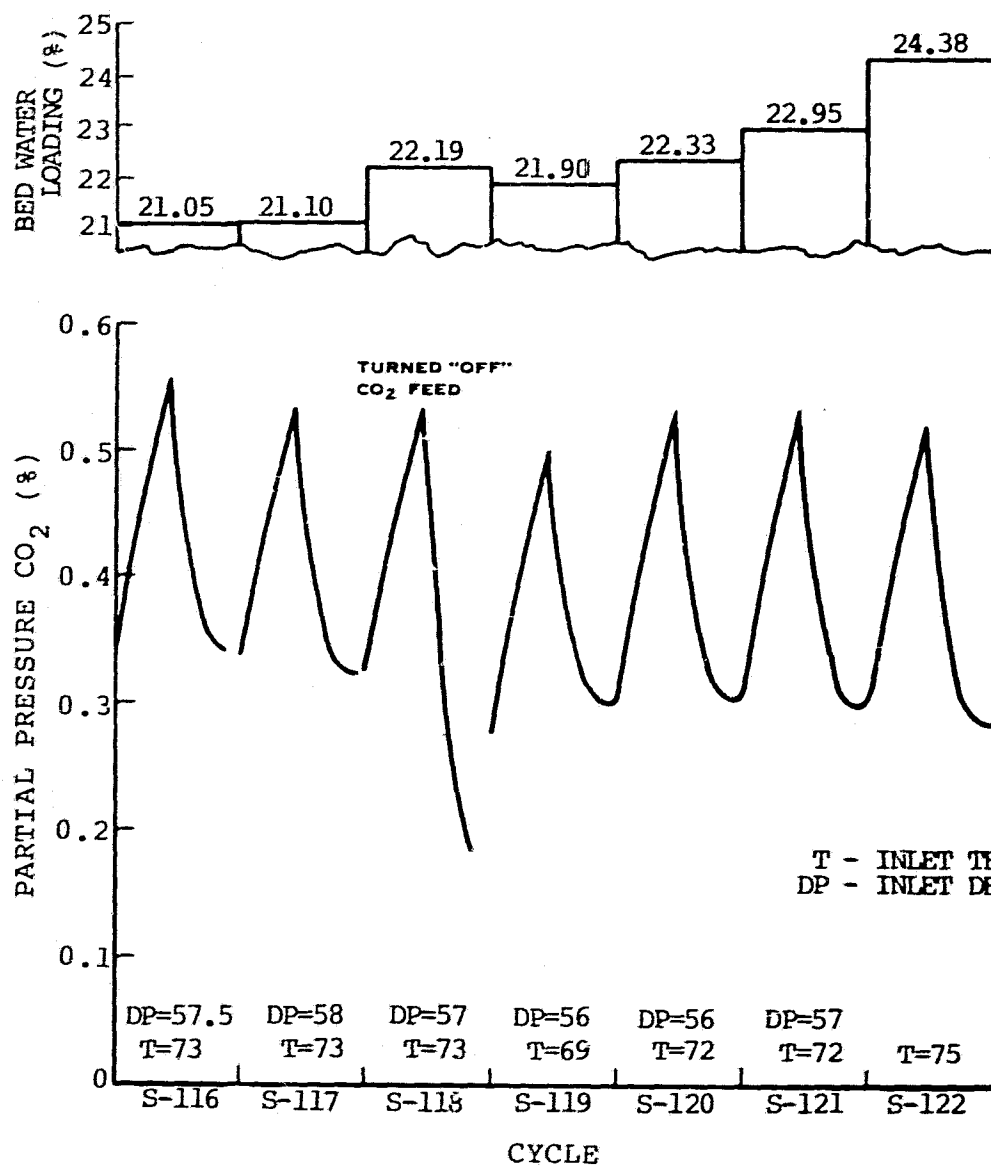


Figure 19  
 SAWD CYCLIC TEST RUNS S-116 - S-122

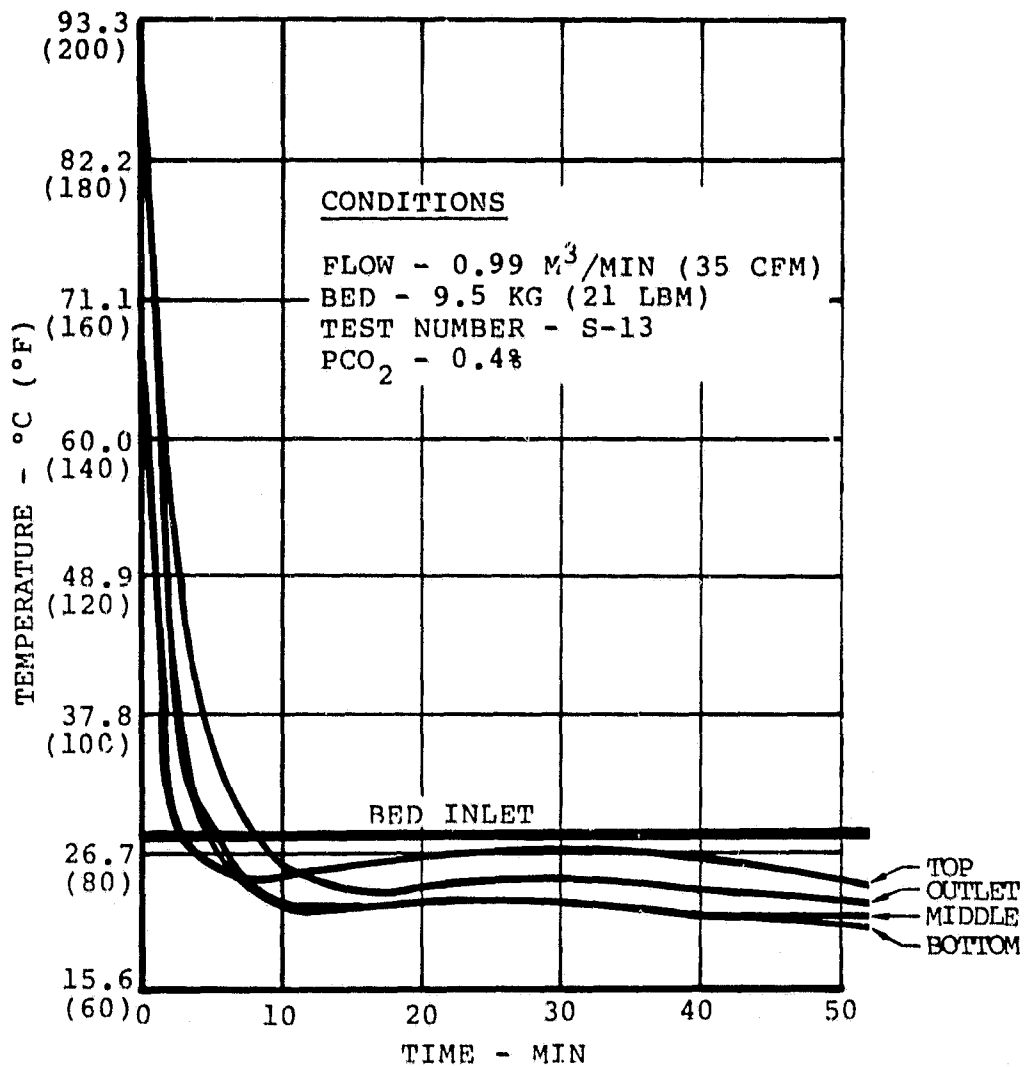


Figure 20  
 BED TEMPERATURE DURING ADSORPTION

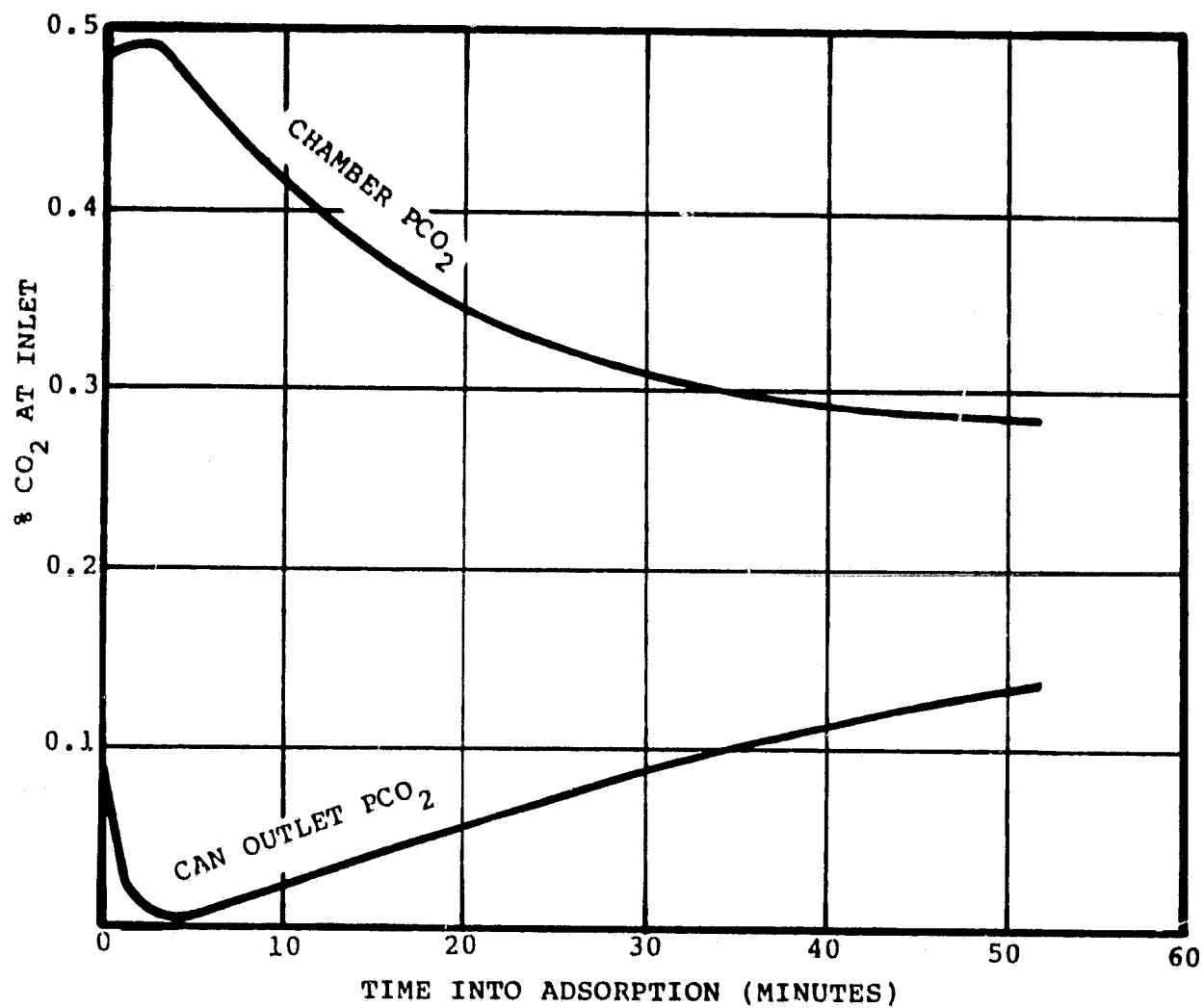


Figure 21

TYPICAL SAWD TEST BREAKTHROUGH CURVE

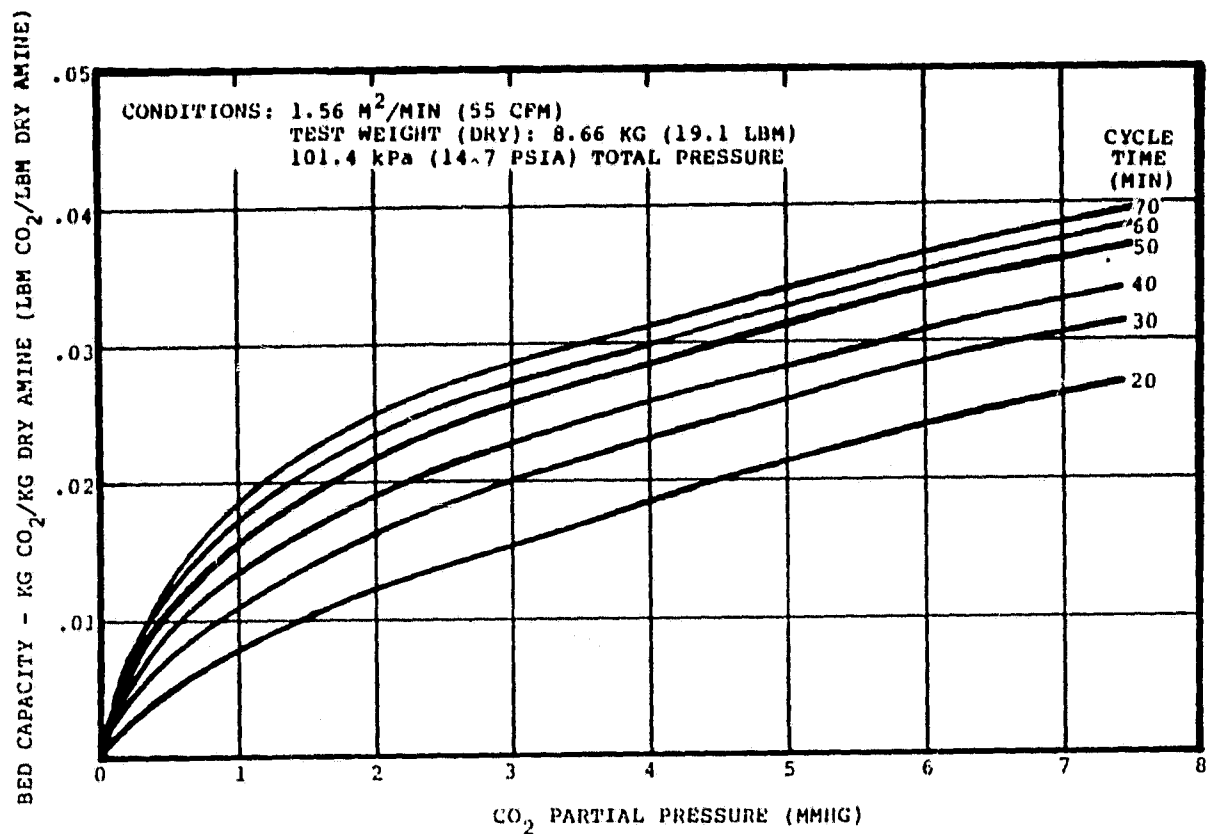


Figure 22  
SOLID AMINE BED CAPACITY AS A FUNCTION OF  
CO<sub>2</sub> PARTIAL PRESSURE AND CYCLE TIME

During some of the initial SAWD test cycles, steam desorption was performed with the bed at a partial vacuum, so that less steam would be required to desorb the bed. Since the bed is heated to the saturated steam temperature, the partial vacuum reduces the temperature to which the bed is heated. Figures 23 and 24 show the adsorption breakthrough and integrated  $\text{CO}_2$  performance curves after desorptions at various temperatures. It is clear that reduced desorption pressures/temperatures cause higher residual  $\text{CO}_2$  loadings on the solid amine. Consequently, adsorption performance is degraded. For desorption at 62.05 kPa (9.0 psia) and 87.22°C (189°F), the cyclic  $\text{CO}_2$  capacity of the solid amine is reduced by 7.3 percent compared to 101.35 kPa (14.7 psia) and 100°C (212°F) desorption. However, even with the increased bed size to account for this reduced performance, the amount of steam required for desorption is less than that required with 100°C (212°F) desorption.

### Bed Drying During Cyclic Operation

Bed drying during the adsorption phase of cyclic operation occurs in two phases. The solid amine bed is an effective heat exchanger. Therefore, during the first few minutes of adsorption, air leaves the bed saturated with water at the average bed temperature. This results in rapid drying and cooling of the bed. The heat of vaporization for the water is drawn from the solid amine material and the bed structure. When the bed temperature approaches the temperature of the inlet air, the second phase of drying begins. Water evaporation rate from the bed is nearly constant and depends on the relative humidity of the inlet air. Sensible heat from the inlet air and heat released by  $\text{CO}_2$  adsorption provide the heat of vaporization for the water. The bed temperature becomes nearly constant slightly above the wet-bulb temperature of the inlet air. Figure 20 shows temperature profiles at various locations in the bed during a typical adsorption cycle. Figure 25 shows the weight change of the bed during an adsorption cycle. The two phases of drying during cyclic SAWD system operation are shown by the bed weight curve without adsorbed  $\text{CO}_2$  weight in Figure 25. It should be noted that if adsorption air flow is continued indefinitely, the bed reaches an equilibrium water content, which is significantly less than the cyclic equilibrium water content with a fixed adsorption cycle.

### $\text{CO}_2$ Desorption From Solid Amine

Solid amine is regenerated by heating it with steam. As the steam is injected into the bed, it condenses releasing its latent heat to the solid amine material and the supporting structure. In this way, the heat progresses through the bed in a well-defined wave. The  $\text{CO}_2$  is desorbed from the heated portion of the bed and readsorbed in the cool downstream portion of the bed. This readsorption can occur, because the  $\text{CO}_2$  partial pressure is much greater than it had been during the adsorption cycle. The solid amine has a significantly greater capacity for  $\text{CO}_2$ , when the  $\text{CO}_2$  is introduced at a higher

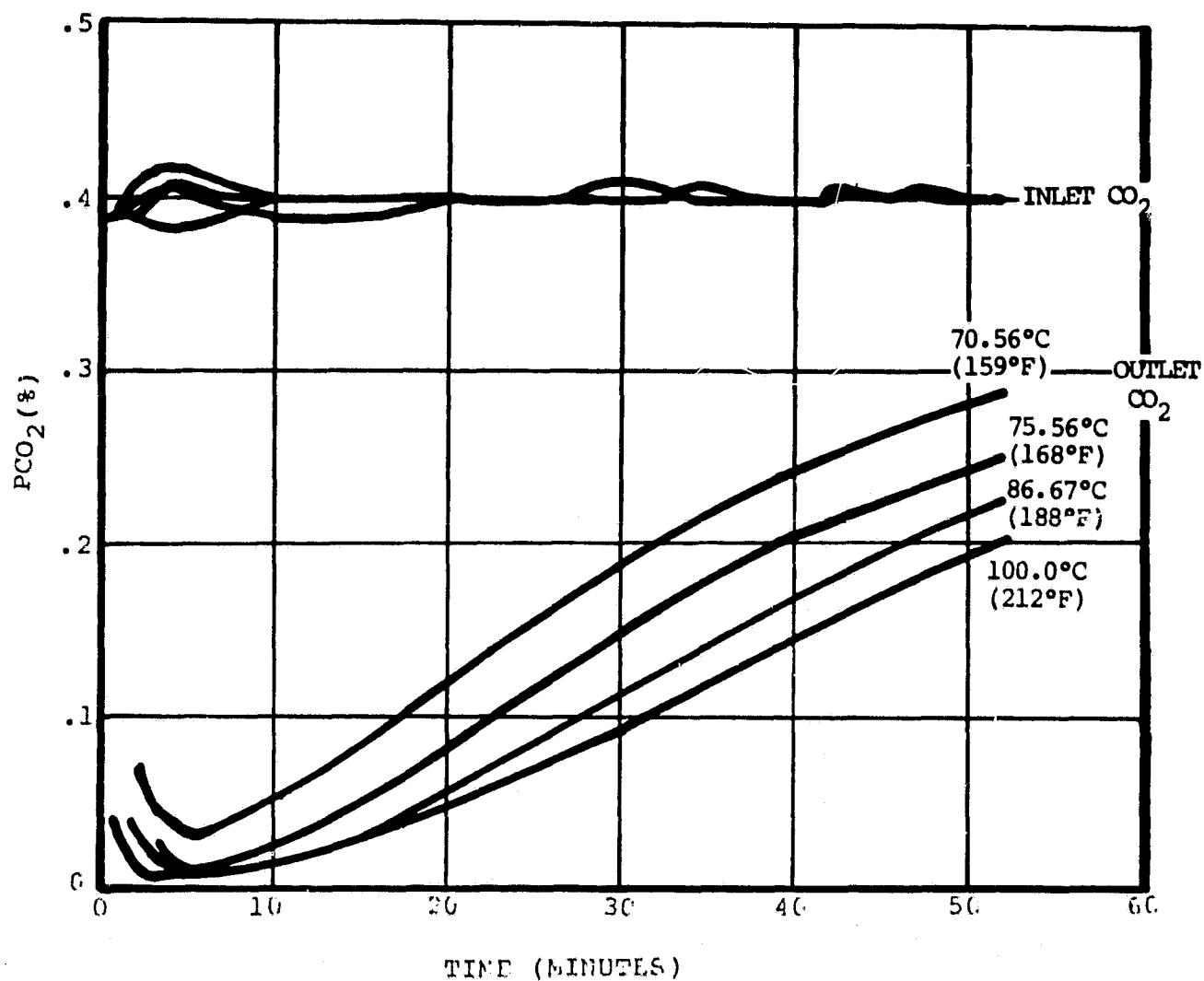


Figure 23  
EFFECT OF DESORB TEMPERATURE  
ON ADSORPTION BREAKTHROUGH

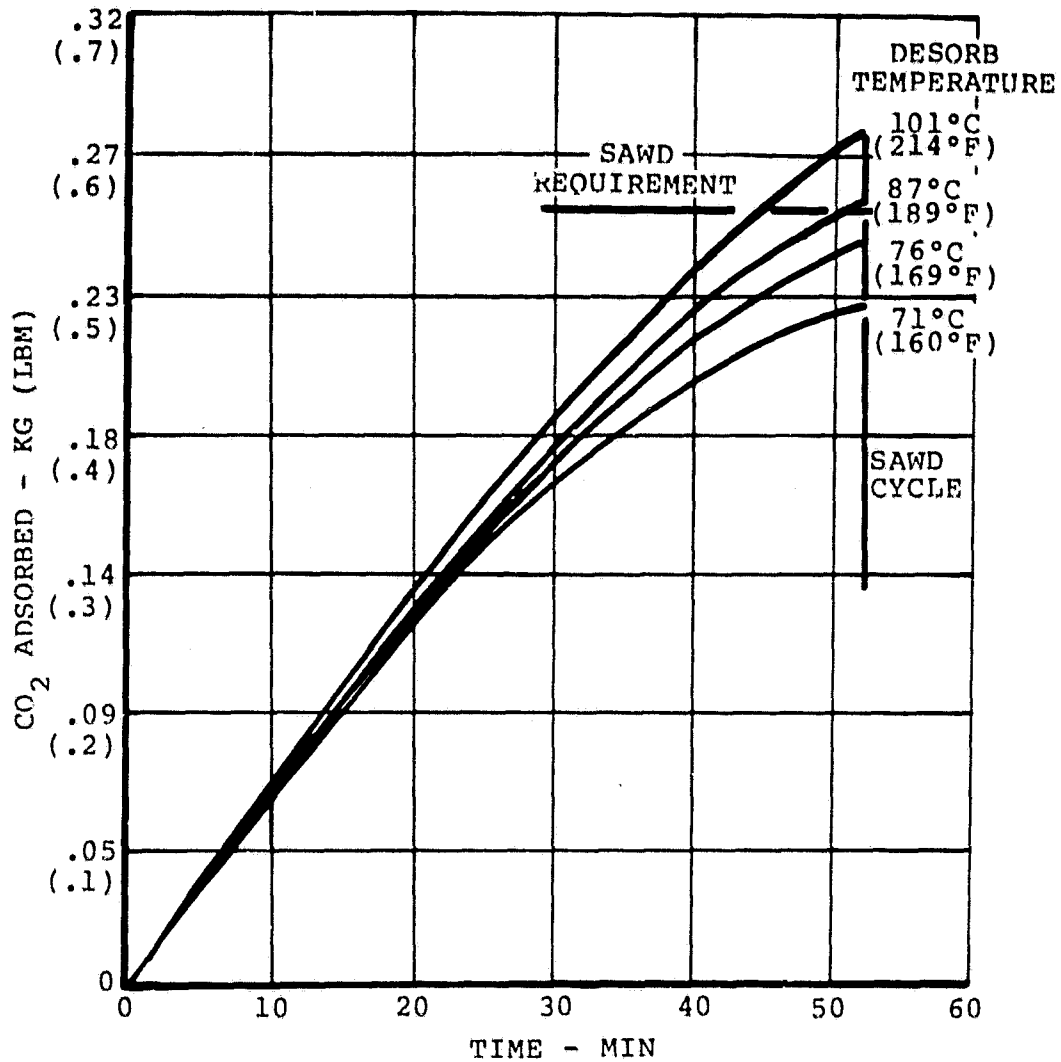


Figure 24  
THE EFFECT OF DESORPTION TEMPERATURE  
ON ADSORPTION PERFORMANCE

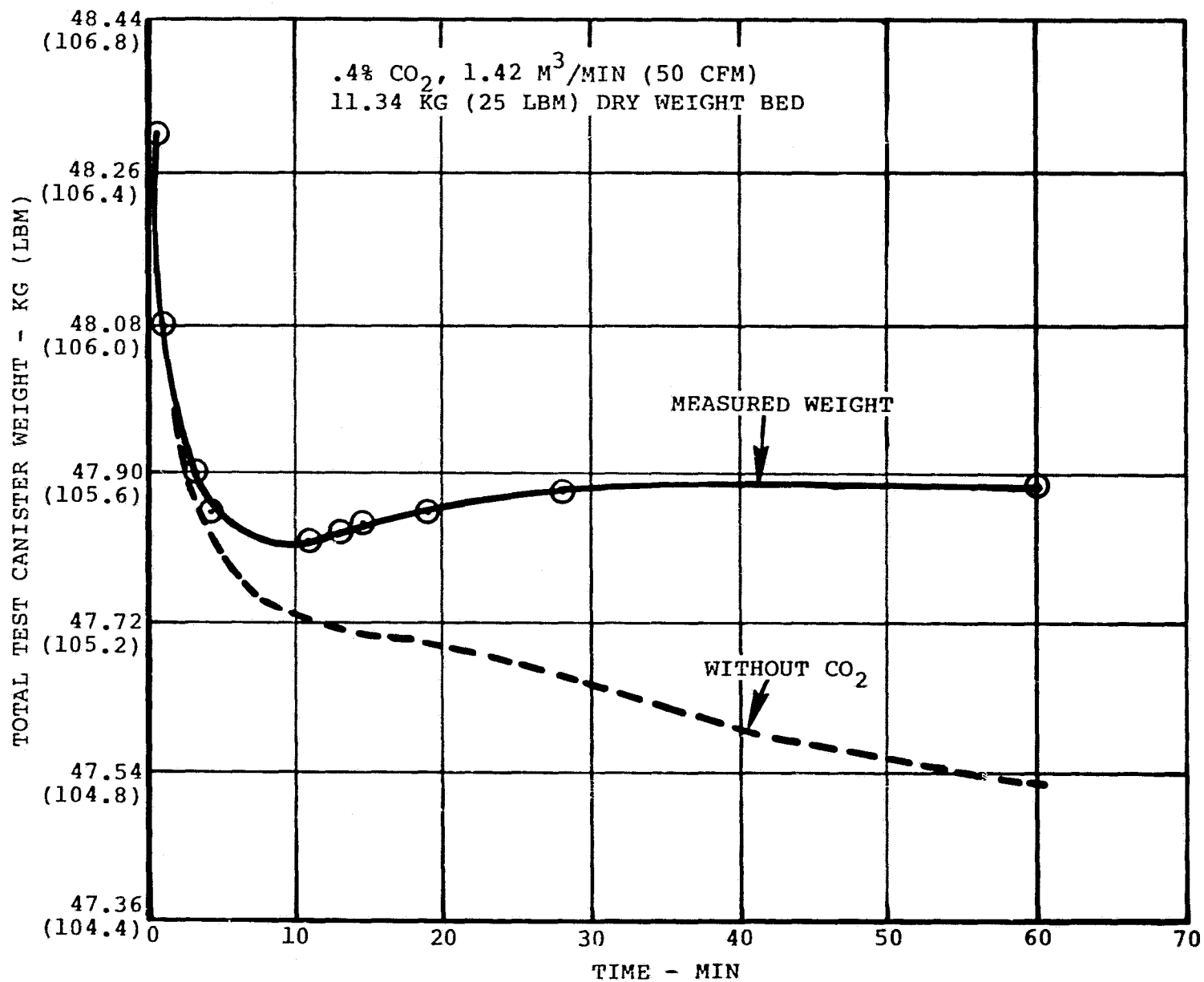


Figure 25  
 SAND CANISTER WEIGHT CHANGE  
 DURING ADSORPTION

partial pressure. This process continues until the remaining unheated section of the bed is fully loaded with  $\text{CO}_2$ . When the steam progresses into this portion of the bed, the desorbing  $\text{CO}_2$  cannot be readsorbed and is pushed out of the bed. Figure 26 shows two  $\text{CO}_2$  desorption profiles from earlier testing. These desorption profiles are from the same solid amine test bed, and they show the effect of different  $\text{CO}_2$  loadings. For the high  $\text{CO}_2$  loading case, the end of the bed becomes saturated sooner, and therefore,  $\text{CO}_2$  is pushed from the bed sooner. However, the maximum  $\text{CO}_2$  flow rate is independent of  $\text{CO}_2$  loading and depends on steaming rate. The small flow during the first part of the desorption is ullage air being displaced by steam from the inlet header and from between the solid amine beads. Figure 27 shows that the rate of bed weight change during desorption is equal to the steaming rate minus the rate at which  $\text{CO}_2$  is driven from the bed.

The steam requirement for desorption is a function of the dry weight of the bed, the  $\text{CO}_2$  loading, and the water content of the bed. For a given system the dry weight of the bed is fixed. Therefore, the steam requirement only varies with  $\text{CO}_2$  loading and water content. For a typical test cycle with a bed water content of 24 percent by weight, there is 2.29 kg (5.04 lbm) of water and 0.254 kg (0.56 lbm) of  $\text{CO}_2$  on the bed. With these values the energy necessary to heat the water from  $21.11^\circ\text{C}$  ( $70^\circ\text{F}$ ) to  $100^\circ\text{C}$  ( $212^\circ\text{F}$ ) is twice the energy required to desorb the  $\text{CO}_2$ . Thus, the most significant factor in the variation of the desorption steam requirement is water content on the bed. Figure 28 verifies this conclusion by showing the strong correlation between the mass of steam required for desorption and the initial bed water content. Similar data is plotted in Figure 29. However, the mass of steam required has been converted to a desorption time using a fixed steaming rate. Figure 30 is a more useful plot of this information. Using Figure 30, the percent of moisture on the bed can be determined from desorption time with a fixed steaming rate.

Further insight into the desorption process was gained by observing the axial temperature distribution of the bed during desorption for low and high  $\text{CO}_2$  loading cases. For the low  $\text{CO}_2$  loading condition Figure 31 shows the expected rapid rise in temperature as the steam reaches each location in the bed. This data shows that the steam progresses through the bed in a well-defined wave. With high  $\text{CO}_2$  loading, Figure 32 shows that the temperature rise at each bed location, except near the bed inlet, begins sooner than it did with the low  $\text{CO}_2$  loading case. The earlier temperature rise occurs because heat of adsorption of  $\text{CO}_2$  is released as the  $\text{CO}_2$  from the upstream portion of the bed is readsorbed. As steam reaches each location in the bed, the temperature rise continues. However, at approximately  $49^\circ\text{C}$  ( $120^\circ\text{F}$ ) the rate of increase is reduced significantly as most of the heat added provides heat of desorption for  $\text{CO}_2$ . Once most of the  $\text{CO}_2$  has been desorbed from one location, the temperature rise continues as in the low  $\text{CO}_2$  loading case. This effect is more pronounced near the end of the bed, because the  $\text{CO}_2$  desorbed closer to the front of the bed has been readsorbed and concentrated near the end.

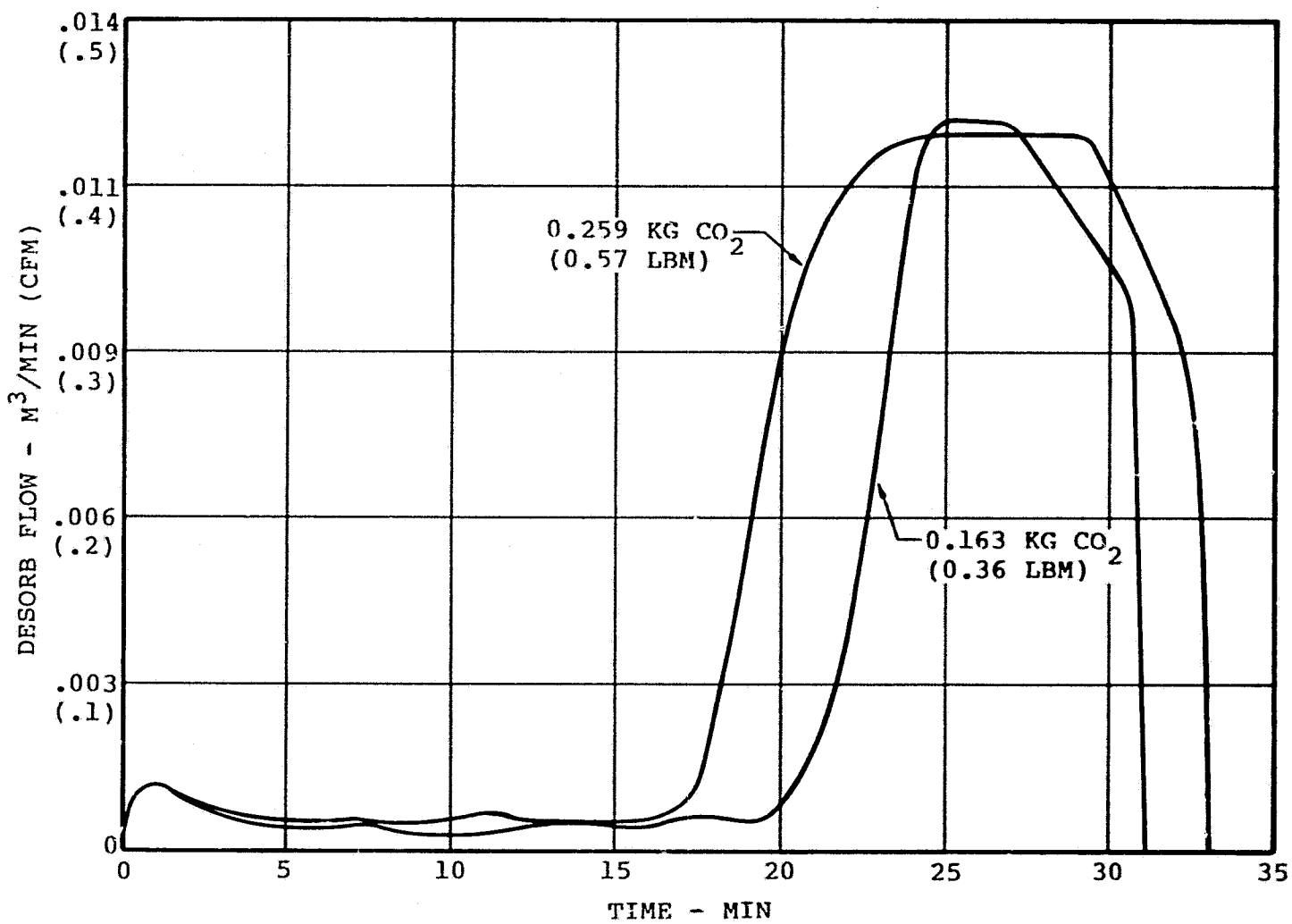


Figure 26  
 EFFECT OF CO<sub>2</sub> LOADING ON  
 DESORPTION FLOW & TIME

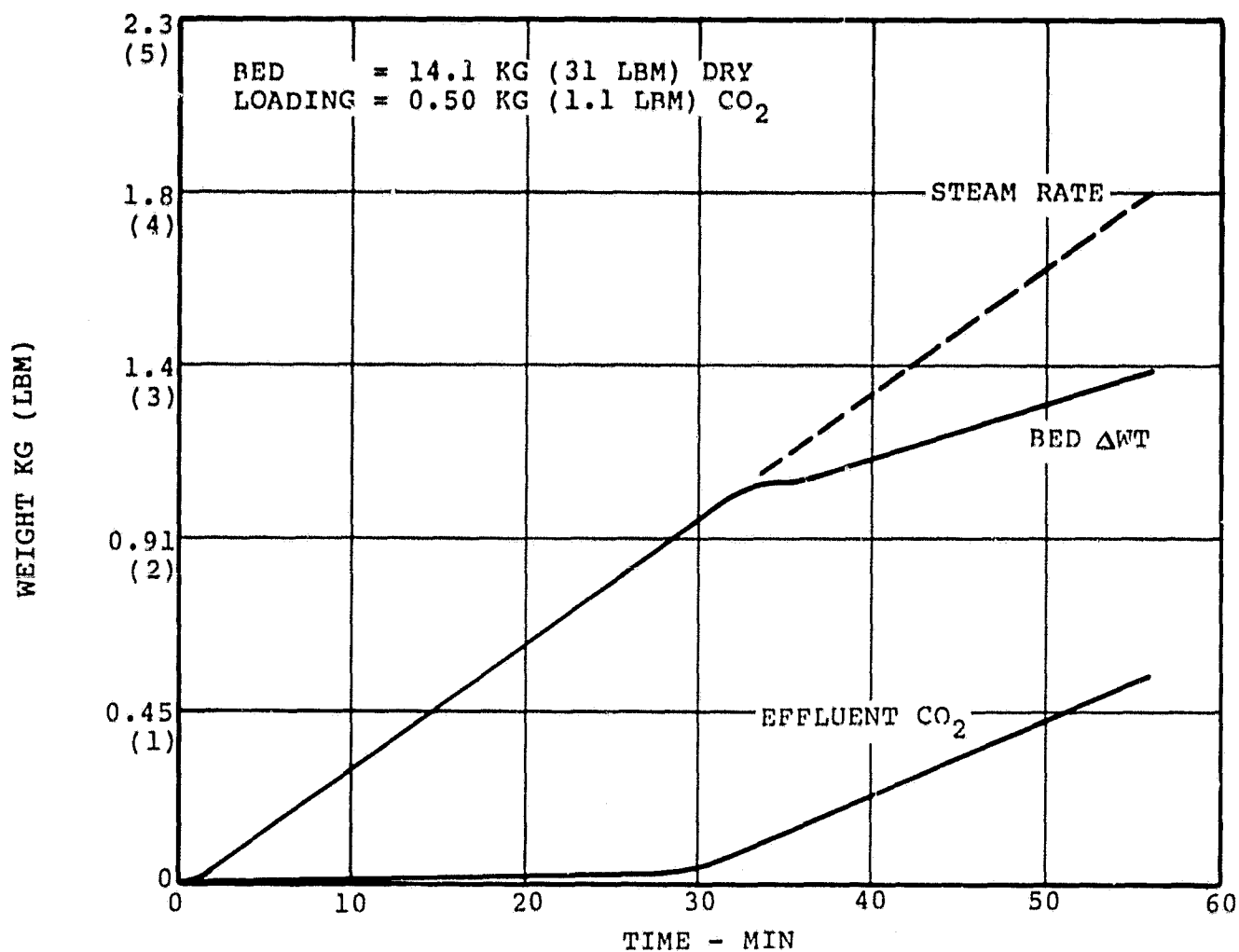


Figure 27  
 DESORPTION MASS CHARACTERISTIC WITH HIGH CO<sub>2</sub> LOADING

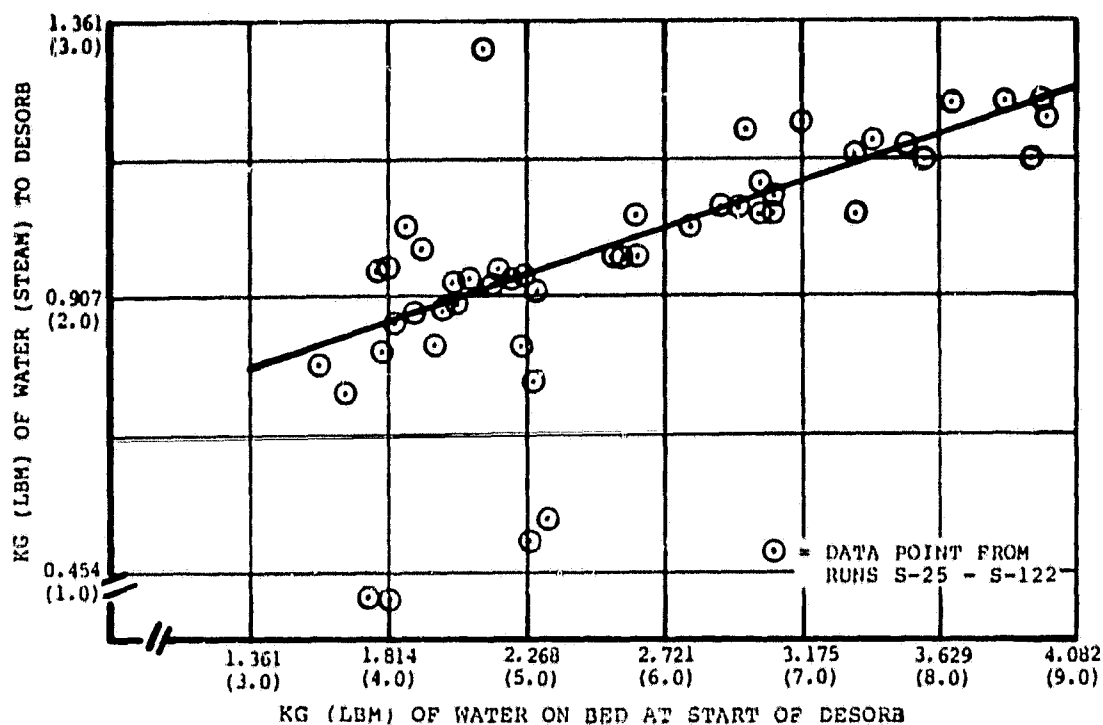


Figure 28

DESORPTION STEAM REQUIREMENTS AS A FUNCTION  
OF BED MOISTURE LEVEL

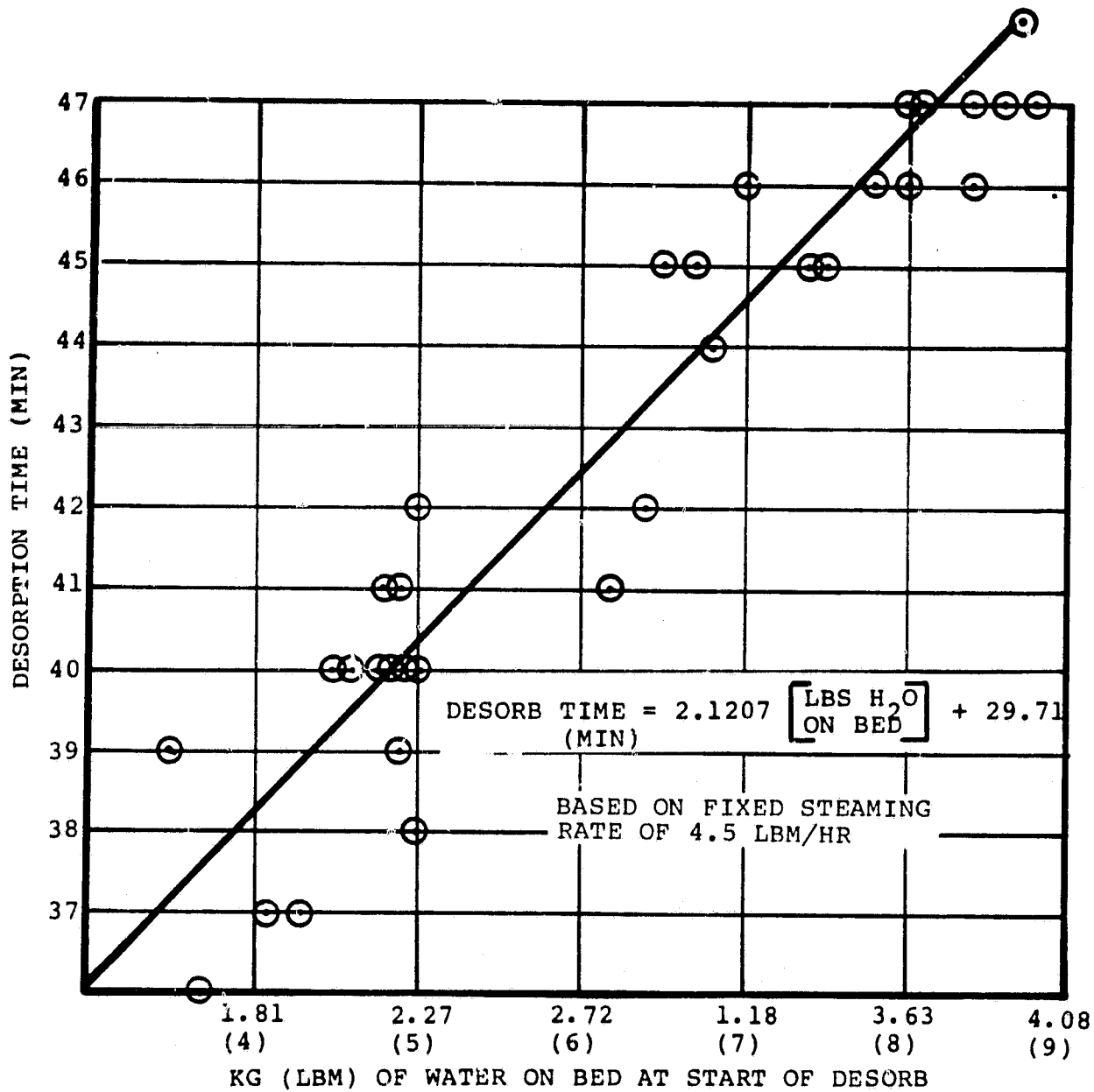


Figure 29  
DESORPTION TIME VS.  
BED WATER LOADING

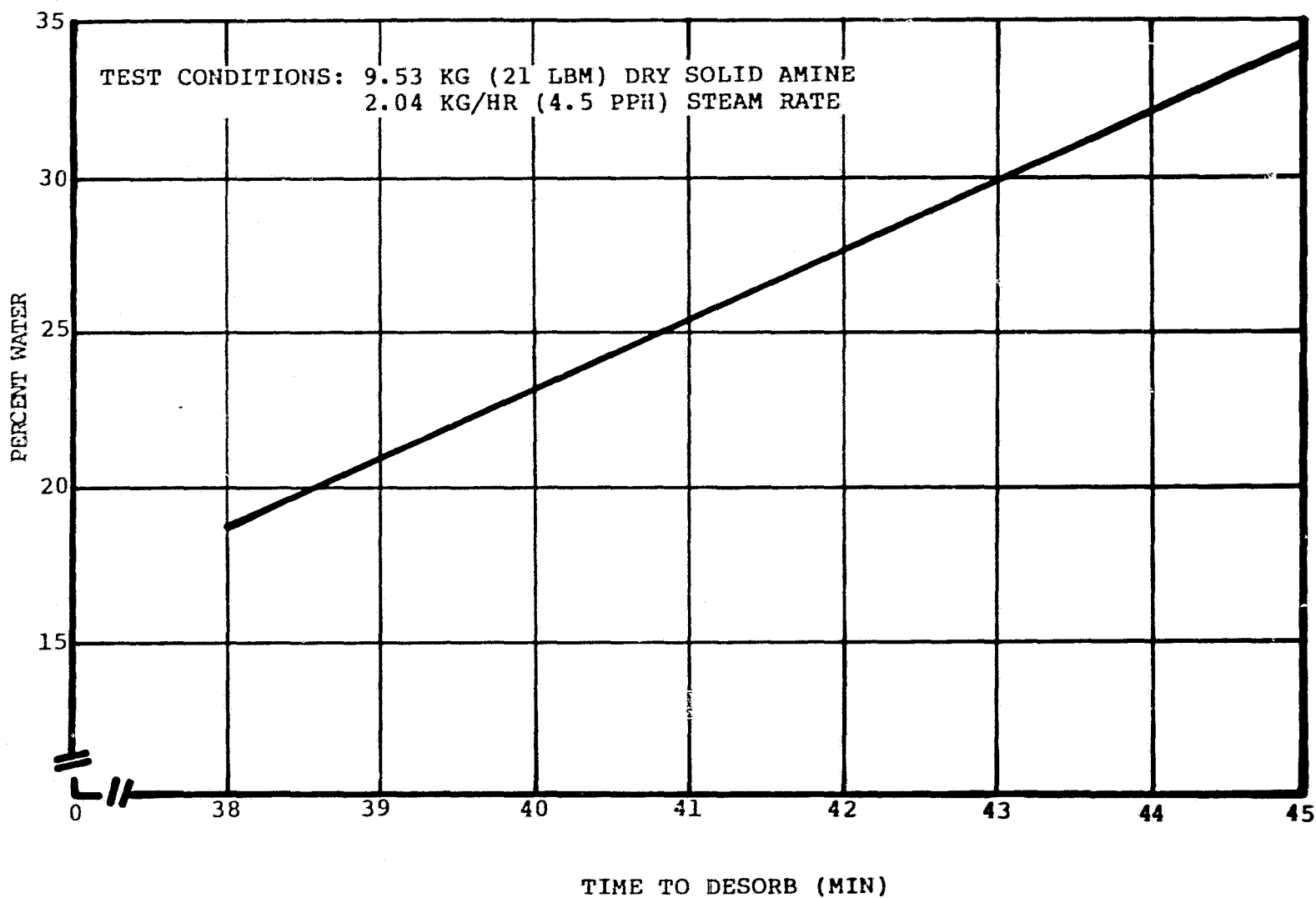


Figure 30  
 PERCENT MOISTURE VERSES DESORPTION TIME

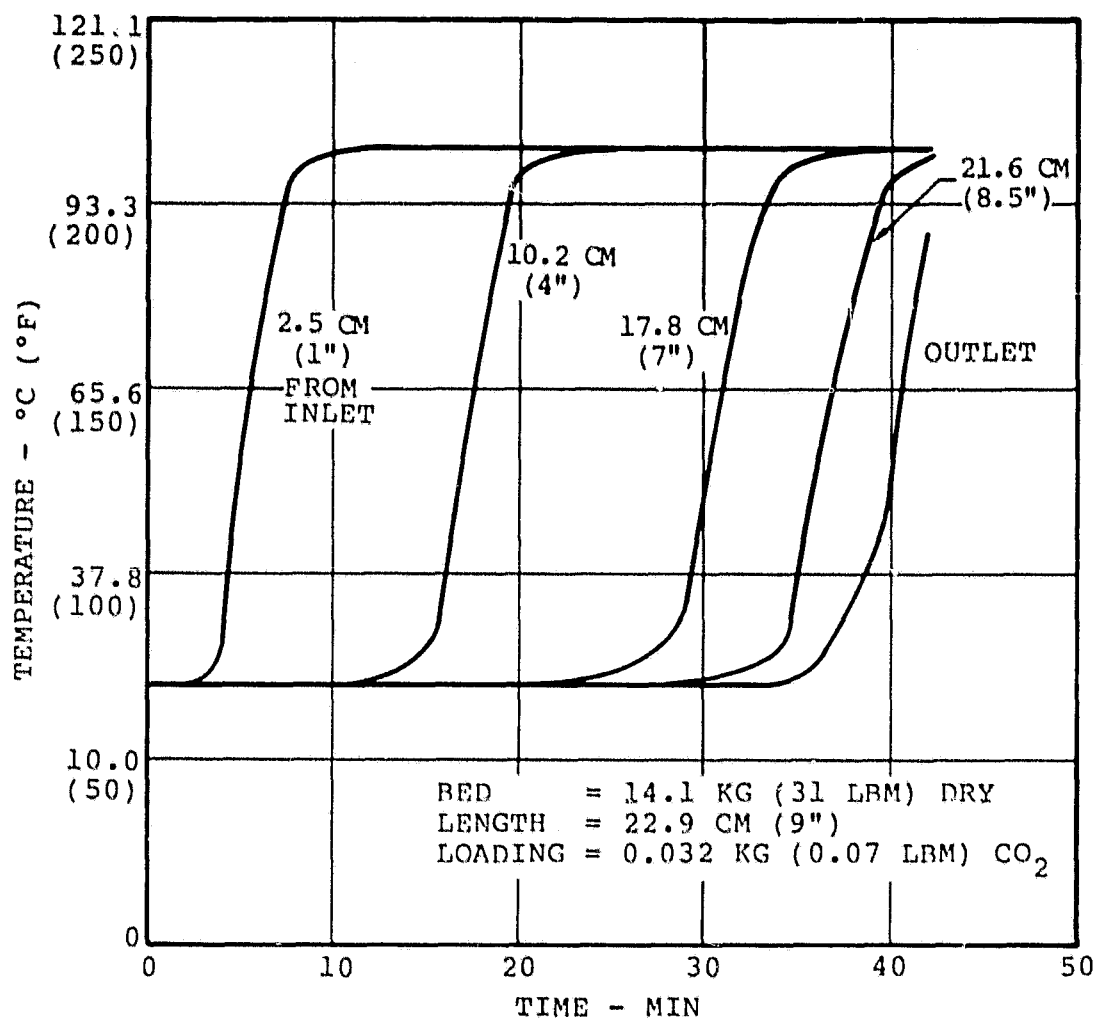


Figure 31

DESORPTION THERMAL CHARACTERISTIC  
 WITH LOW CO<sub>2</sub> LOADING

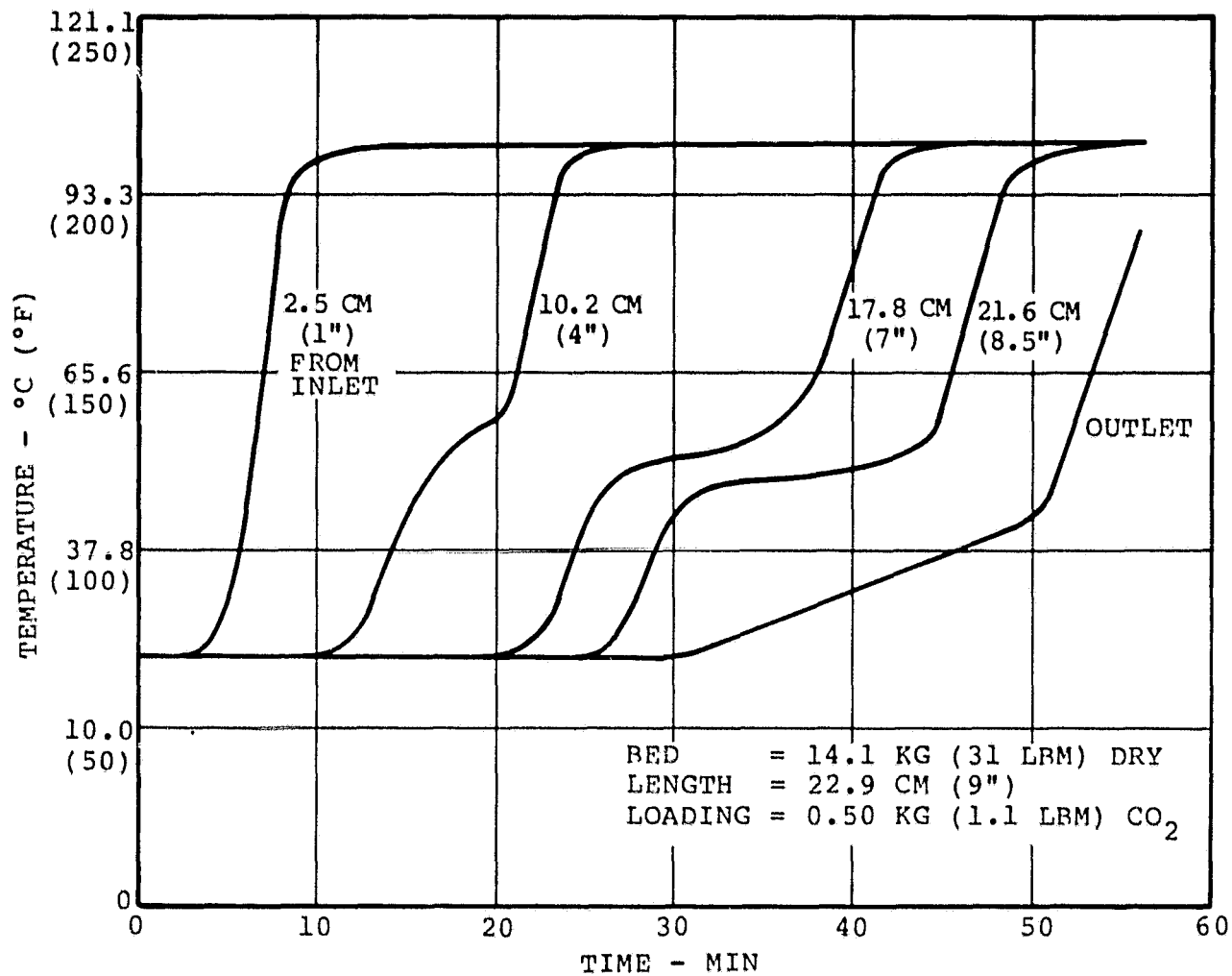


Figure 32  
DESORPTION THERMAL CHARACTERISTIC WITH HIGH CO<sub>2</sub> LOADING